UNIVERSITI MALAYSIA PAHANG

DECLARATION OF THESIS / UNDERGRADUATE PROJECT PAPER AND COPYRIGHT

Author's full name: **VIKNESH A/L PUNICHELVAN**

Date of birth : **3RD JANUARY 1989**

Title : **DESIGN AND IMPLEMENTATION OF FLYWHEEL ENERGY STORAGE SYSTEM FOR SUPPORTING CRITICAL LOAD**

Academic Session : **2012/2013**

I declare that this thesis is classified as:

☐	**COFIDENTIAL**	(Contain confidential information under the Official Secret Act 1972)*
☐	**RESTRICTED**	(Contains restricted information as specified by the organization where research was done)*
√	**OPEN ACCESS**	I agree that my thesis to be published as online open access (full text)

I acknowledge that Universiti Malaysia Pahang reserves the right as follows:

1. The Final Year Project Report is the property of Universiti Malaysia Pahang.
2. The Library of UniversitI Malaysia Pahang has the right to make copies for the purpose of research only.
3. The library has the right to make copies of the thesis for academic exchange.

Certified by:

Viknesh

SIGNATURE | **SIGNATURE OF SUPERVISOR**

890103-14-5673
(NEW IC NO./ PASSPORT NO.)

PROF.MADYA. DR. AJISMAN APEN

Date: **28 JUNE 2013**

Date: 4/7 - 2013

NOTES: * If the thesis is CONFIDENTIAL or RESTRICTED, please attach with the letter from the organization with period and reasons for confidentiality or restriction

DESIGN AND IMPLEM[illegible] ERGY STORAGE SYSTEM FOR SUPPORTING CRITICAL LOAD

VIKNESH A/L PUNICHELVAN

Thesis submitted in partial fulfilment of the requirements for the award of the degree of Bachelor of Mechatronics Engineering

Faculty of Manufacturing Engineering
UNIVERSITI MALAYSIA PAHANG

JUNE 2013

UNIVERSITI MALAYSIA PAHANG

FACULTY OF MANUFACTURING ENGINEERING

I certify that the project entitled "Design and Implementation of Flywheel Energy Storage System for Supporting Critical Load" is written by Viknesh Punichelvan. I have examined the final copy of this thesis and in my opinion; it is fully adequate in terms of scope and quality for the award of the degree of Bachelor of Mechatronics Engineering. I herewith recommend that it be accepted in fulfillment of the requirements for the degree of Bachelor of Mechatronics Engineering.

(ASSOC. PROF.DR.ABDUL AZIZ BIN JAAFAR)
Examiner

Signature:

SUPERVISOR'S DECLARATION

I hereby declare that I have checked this project and in my opinion, this project is adequate in terms of scope and quality for the award of the degree of Bachelor of Mechatronics Engineering.

Signature:
Name of Supervisor: ASSOCIATE PROFESSOR DR. AJISMAN APEN
Position: LECTURER OF FKP
Date: 4/7-2013

STUDENT'S DECLARATION

I hereby declare that the work in this project is my own except for quotations and summaries which have been duly acknowledged. The project has not been accepted for any degree and is not concurrently submitted for the award of other degree.

Signature:

Name: VIKNESH A/L PUNICHELVAN

ID Number: FB09002

Date: 28 JUNE 2013

Dedicated to my parents, sisters, family members and friends who have directly or indirectly contributed for the completion of this project paper.

ACKNOWLEDGEMENTS

I'm grateful and would like to express my heartfelt gratitude to my parents, brother and sisters for their love, sacrifice, encouragement and support which made the completion of this paper possible. Without them, I could not have achieved something this meaningful in my life.

Hereby, I also acknowledge my sincere indebtedness and gratitude to express my heartfelt gratitude to my supervisor, Associate Professor Dr. Ajisman Apen for his brilliant ideas, invaluable guidance, incessant encouragement and relentless support in making this research possible. He has always impressed me with her outstanding passion for study in reaction and analysis. I undertook this topic from this field to be studied with much interest that I believe I have gained from him. He, not only my final year project supervisor, was also my Power Electronics and Electrical Drive System lecturer who has guided me and provided his continuous support for these subjects. I am also truly grateful for him progressive vision about my study about liquid systems, his tolerance of my mistakes.

My sincere thanks also goes to all lab staffs of Faculty of Manufacturing Engineering, UMP who have also continuously supported and educated me throughout the way. Hereby, I also acknowledge my sincere indebtedness and gratitude to my parents and sisters for their love, sacrifice, encouragement and support which made the completion of this paper possible. Without them, I could not have achieved something this meaningful in my life.

ABSTRACT

Flywheel energy storage system (FESS) is a system that can store energy in mechanical form and release out in electrical form. Nowadays, energy storage systems were widely used such as battery, hydroelectric, fossil fuels and also flywheel energy storage. The main principle of flywheel is the more energy that enters the systems the faster it rotates. The aim of this study is to design and implement a FESS for critical load. Then, period of power generated by FESS was analyzed. Besides that, the voltage that generated by FESS was compared based on minimum value of capacitance used in self excited generator (SEIG). Firstly, a thin firm shaped flywheel rotor was fabricated and it was assembled to the SEIG. FESS consists of a self-excited capacitance induction motor-generator set, power exchange circuit and flywheel rotor. When, there is an ac source, the flywheel rotor start to rotate and it stores energy. Then, the stored energy can be released to the critical load when blackout occurs. The energy stored in the system depends on the properties and moment of inertia of flywheel rotor. The obtained result indicated 47μF is the suitable minimum value of the capacitance of SEIG, and it followed by 33μF and 68μF. The result shows FESS potential to store energy for short period. This study can be a significant initiation to an energy storage system.

ABSTRAK

Sistem roda tenaga adalah satu sistem penyimpanan tenaga yang boleh menyimpan tenaga dalam bentuk mekanikal dan melepaskan dalam bentuk elektrik. Pada masa kini, sistem penyimpanan tenaga telah digunakan secara luas seperti bateri, hidroelektrik, bahan api fosil dan juga roda tenaga penyimpanan tenaga. Prinsip utama roda tenaga adalah apabila lebih bantak tenaga memasuki sistem, pemutaran roda tinggi juga meningkat. Tujuan kajian ini adalah untuk merekabentuk dan melaksanakan sistem roda tenaga untuk beban kritikal. Kemudian, tempoh kuasa yang dihasilkan oleh sistem roda tenaga telah dianalisis. Selain itu, voltan yang dihasilkan oleh sistem roda tenaga telah dibandingkan berdasarkan nilai minimum yang digunakan dalam penjana teruja diri (SEIG). Pertama, sebuah roda tenaga yang berbentuk silinder direka dan telah dipasang pada SEIG. sistem roda tenaga terdiri daripada pemuat sendiri teruja induksi set motor-penjana, litar pertukaran kuasa dan roda tenaga pemutar. Apabila, tenaga elektrik dialir ke sistem roda tenaga, roda tenaga pemutar mula berputar dan ia menyimpan tenaga. Kemudian, tenaga yang disimpan boleh dikeluarkan kepada beban kritikal apabila blackout berlaku. Tenaga yang disimpan di dalam sistem bergantung kepada sifat dan momen inersia roda tenaga pemutar. Keputusan yang diperolehi menunjukkan 47μF adalah nilai minimum yang sesuai kapasitan SEIG, dan ia diikuti oleh 33μF dan 68μF. Hasilnya menunjukkan sistem roda tenaga potensi untuk menyimpan tenaga untuk tempoh yang singkat. Kajian ini boleh menjadi permulaan yang ketara kepada sistem penyimpanan tenaga.

TABLE OF CONTENTS

LIST OF TABLES

LIST OF FIGURES

Page

LIST OF SYMBOLS

E_k	Kinetic energy
I	Moment of inertia
ω	Angular velocity
e_v	Kinetic energy per unit volume
e_m	Kinetic energy per unit mass
K	Shape factor of flywheel
σ	Maximum stress
ρ	Mass density
ω_m	Rotor speed in radians per seconds
ω_s	Synchronous speed in radians per seconds
n_{sync}	Synchronous speed in revolution per minutes
n_m	Rotor speed in revolution per minutes
f_e	Frequency
P	Number of Poles
s	Percentage of slip
P_{conv}	Induced power
τ_{ind}	Induced torque
P_{loss}	Mechanical loss
P_{cu}	Copper loss
P_{wind}	Windage loss
V	Voltage
μF	Microfarad
kW	Kilowatt
ds	Deciseconds

LIST OF ABBREVIATIONS

FESS	Flywheel energy storage system
UPS	Uninterruptible power source
AC	Alternative current
SEIG	Self excited induction generator
CAD	Computer-aided design
CAM	Computer-aided manufacturing
RPM	Revolution per minute
NC	Numerical control
SPDT	Single pole double throw

CHAPTER 1

INTRODUCTION

This chapter mainly emphasizes on the general idea of this study along background of study, problems identification and objectives of the project and scope of work that must be done.

1.1 BACKGROUND OF THE STUDY

Storing energy plays an important role in human's life to balance the supply and demand of energy. The energy storage system that currently used can be categorized as mechanical, electrical, chemical, biological and also thermal. Nowadays, there are so many energy storage systems were widely used such as battery, hydroelectric, fossil fuels and also flywheel energy storage. Not all this energy storage systems technically and economically feasible. Flywheel energy storage system (FESS) stored energy in mechanical form. It stored the kinetic energy in the spinning flywheel. Development in material technology, power electronic and signal electronic becomes flywheel as a promising candidate for the energy storage system.

Thousand years ago, the flywheel has been utilized. Then, a few hundred years ago mechanical flywheels where widely used to achieve smooth operation of machines from cycle to cycle, thereby render possible the industrial revolution. The early models flywheels consisting of only a stone wheel attached to an axle. Then, in the 1970s the flywheel energy storage was proposed as a primary objective for electric vehicles and stationary power backup. On the same time, fiber composite rotors where built and magnetic bearings were started to appear in the 1980s. Thus the potential for using flywheel as electric energy storage has long been established by extensive research. Nowadays flywheels widely used to store energy mechanically and transferred to electrical energy. FESS can have energy fed in the rotational mass of a flywheel, store it as kinetic energy, and release out up on demand (Bolund, B., Bernhoff, H., & Leijon, M., 2007).

The main principle of flywheel is the more energy that enters the systems the faster it rotates. So, the system can be stored more energy in form of mechanical. The FESS which works by accelerating a cylindrical assembly called a rotor to a very high speed and maintaining the energy in the system as rotational energy. This rotational energy is converted back by slowing down the flywheel. The most advanced flywheel energy storage system consists of blades made of composite materials and magnetic bearings that rotate at speed of 20,000 to 50,000 revolutions per minute. This kind of systems can maximally stored energy in few minute and have energy efficiency up to 90 percent. The ration of energy that can be taken out of the system in relation to the energy supplied to the system is called as energy efficiency.

Recently, flywheel is proving to be an ideal form of storage on account of its high efficiency, long cycle life, wide operating temperature range, freedom from depth of discharge effects and higher power and energy density on both a mass and a volume basis (Liu, H., & Jiang, J., 2007). Nowadays, effective saving energy has developed for leveling energy consumption between day-time and night time, preventing instantaneous voltage change. A FESS is one of valuable energy-saving system. When compared to other energy storage systems, FESS is very simple and characterized by high energy density (Murakami, K., Komori, M., Mitsuda, H., & Inoue, a., 2007).

FESS has lot of advantages. One of the most valuable advantages of FESS is producing critical emergency power supply for limited period. Nowadays, flywheels are widely used as supplementary uninterruptible power source (UPS) or flywheel backup at several industries especially industries that depend on computers works. This is because; the data that stored in computers might loss when there is sudden power off. So, a flywheel can produce electrical power to a computer room for a few minutes or hours. Flywheels also have some other advantages such as it can operate at a much wider temperature range, not affected by temperature changes and are not subject to many of the common failures of chemical rechargeable batteries. More than, a flywheel system itself is a kinetic or mechanical battery, spinning at very high speeds to store energy that is instantly available when needed. Another major advantage of flywheels is the ability to handle high power levels. For example, this is a desirable quality in a vehicle, where a large peak power is necessary during acceleration (Bolund, B., Bernhoff, H., & Leijon, M., 2007).

In this study, the FESS for a critical load will discussed. The output of the flywheel energy storage system is discussed. Then, the possibility of using different value of capacitance in self excited induction generator (SEIG) is also discussed.

1.2 PROBLEM STATEMENT

Mostly the normal power system could not full fill the requirement for the critical load. There are many critical loads such as computer rooms, operation rooms in hospitals are immediately need high reliability and quality of power supply. A sudden power shut down, can bring lot of negative impacts such as data lost, delay and also to a human's life. So, an energy storage system is a best solution that can be solved this problem. A FESS which stored energy in the mechanical form would be able to support the critical loads for a short period.

1.3 OBJECTIVES

There are a few objectives that one would like to achieve at the end of this study. The main objective of this study is to design and implement a FESS for critical load by using self excited induction machine (SEIG). Then, to analyze the period of power that produced by the FESS to the supporting critical load. Besides that, another objective of this study is to determine the voltage generated by FESS for different value of capacitance.

1.4 SCOPE OF STUDY

This study aim to use thin firm shaped flywheel in FESS. Then, aluminium was chose as raw material for the flywheel rotor. Another scope of this study is using a three phase asynchronous induction machine as motor-generator set of FESS.

CHAPTER 2

LITERATURE REVIEW

2.1 FLYWHEEL BASICS

2.1.1 Energy storage system in Flywheels

Flywheel is acting as the medium carrying energy. The inertia of a rotating mass used to store energy in a flywheel. The amount of kinetic energy that stored as rotational energy is depending on the inertia and speed of rotating mass (Jiancheng et al., 2002). Normally, the flywheel is placed in a vacuum chamber to reduce or eliminate the friction-loss from the air and suspended by bearings for stabile operation. The kinetic energy is transferred and out of the flywheel with an electrical machine that can function either as a motor or generator. When that electrical machine acts as a motor, the electric energy supplied to the stator winding is converted to torque and applied motor, causing it to spin faster and gain kinetic energy. While in the generator mode, kinetic energy stored in the rotor applies a torque that converted to electric energy.

The kinetic energy that stored in the thin firm flywheel is proportional to the mass and to the square of its rotational speed according to Eq. (2.1).

$$E_k = \frac{1}{2} I\omega^2 \tag{2.1}$$

Where E_k is kinetic energy stored in the flywheel. I is moment of inertia and ω is the angular velocity of the flywheel. The moment of inertia is a function of its shape and mass (Bolund.B et al., 2007). Eq. (2.1) shows that the way to increase the stored energy is to speed up the flywheel.

The speed limit is set by the stress developed within the wheel due to inertial loads, called tensile strength σ. The lighter material which develops lower inertial loads at a given speed with low density and high tensile strength is good for storing kinetic energy. The maximum energy density respect to volume and mass respectively is:

$$e_v = K_\sigma \tag{2.2}$$

$$e_m = K\sigma/\rho \tag{2.3}$$

where e_v is kinetic energy per unit volume , e_m is kinetic energy per unit mass, K is shape factor, σ is maximum stress in the flywheel and ρ is mass density (Kirk, J. A., 1977). Since the energy stored is proportional to the square of angular velocity, increasing the angular speed is more effectively than increasing mass to increase the stored energy. But a rapid increasing of angular speeds will cause increase in frictional losses and also thermal problems. So, in such cases, the magnetic bearing technology used to reduce the frictional losses, but it's too expenses (Thesis, A., 2003). Table 2.1 shows that the shape-factor for different planar stress geometries.

Table 2.1: Shape-factor K for different planar stress geometries

Fly wheel geometry	Cross section	Shape factor K
Disc		1.000
Modified constant stress disc		0.931
Conical disc		0.806
Flat unpierced disc	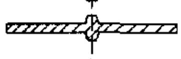	0.606
Thin firm	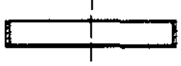	0.500
Shaped bar		0.500
Rim with web		0.400
Single bar	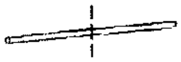	0.333
Flat pierced bar	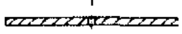	0.305

Source: Bolund.B et al., (2007)

2.1.2 Flywheel Materials

The flywheel can be divided into two classes, which based on material in the rotor. For first class of flywheel advanced composite materials used to made up the rotor. These kinds of the materials have very high strength to weight ratios that bring high specific energy to the flywheels. Overall, these classes of flywheels determine the performance of flywheels. The maximum stored energy is ultimately limited by the tensile strength of the flywheel material. Fiber composites are the better choice for FESS. Table 2 illustrates theoretical flywheel energy comparison when K = 0.5. Composite materials is highest tensile when compares to the steel material.

Table 2.2: Data for different rotor materials

Rotor material	σ_m (GPa)	ρ (kg/m^3)	E_{sp} (Wh/kg)
E-glass	3.5	2540	190
S-glass	4.8	2520	265
Kevlar	3.8	1450	370
Spectra 1000	3.0	970	430
T-700 graphite	7.0	1780	545
T-1000 graphite (projected)	10.0	–	780
Managing steel	2.7	8000	47

Source: Liu, H., & Jiang, J. (2007)

2.2 MOTOR / GENERATOR

In the FES system, the motor/generator is used to exchange the electric energy and kinetic energy. The motor/generator acted as a motor and the flywheel accelerates, when the flywheel stores energy. While the motor/generator acts as generator, the flywheel releases the energy. So the generator will produce an electrical power to the load. Normally, in a simple FESS the asynchronous motor used as motor/generator because this kind of motor easy to be built for high power and easy to operate at high speed. It's easy to be driven by the AC power converter (Jiancheng et al., 2002). Overall, it can be said that, the motor/generator and power electronic determines the power capabilities if the system.

2.2.1 Induction Machine

According to Stephen J. Chapman (2002), induction machine is a machine that with only amortisseur windings. Induction machine also is a kind of AC motor where power is supplied to the rotor by electromagnetic induction which means the voltage is induced in the rotor windings instead of being physically connected by wires. There are two different types of induction machine rotors, which are squirrel cage rotor and wound rotor. In this study, a three phase squirrel cage rotor induction machine was used. A squirrel-cage induction machine rotor consists of a series of conducting bars laid into slots carved in the face of the rotor and shorted at either end by large shorting rings.

An induction machine is possible to function as either as a motor or as a generator when it connected to an ac source of appropriate voltage and frequency. Regeneration is possible, if the rotor of the induction machine is able to rotate above synchronous speed decided by supply frequency and the pole number of the machine (Singh, G. K., 2004). When the induction machine acts as a motor, the rotor speed of the motor, ω_m will be less than the synchronous speed, ω_s. So, the rotor effectively moves in clockwise direction with respect the magnetic field, inducing in each bar a voltage having the polarity indicated and a magnitude proportional to slip velocity and to the field strength acting on the bar. While, in a generator mode, the rotor speeds of motor, ω_m is faster than the synchronous speed, ω_s (Mahmoud Riaz., 2010). Then the direction of the induced torque in the machine reverses and the machine becomes generator, converting mechanical power to electric power (Stephen J. Chapman., 2002). The synchronous speed and the rotor speed of the motor respectively can be calculated by equations;

$$\text{Synchronous speed, } n_{sync} = \frac{120 f_e}{P} \tag{2.4}$$

$$\text{Rotor speed, } n_m = (1 - s)n_{sync} \tag{2.5}$$

Where, f_e is the system frequency in Hertz and P and s are the number of poles in the machine and percentage of slip in the machine. The power converted to mechanical form in an induction motor is equal to;

$$\text{Induced power, } P_{conv} = \tau_{ind}\,\omega_m \tag{2.6}$$

Where, τ_{ind} is an induced torque in an induction machine. The speed of an induction motor can be accomplished by changing the number of poles on the machine, by applied electrical frequency and by changing the applied terminal voltage.

2.2.2 Self-Excited Induction Generator (SEIG)

In recent years, squirrel cage induction machines are used as the electromechanical energy converter. The principle of self-excitation applied to the induction machines to generate electricity. According to Tze-Fun (1888), an induction machine called as self-excited induction generator (SEIG), when a suitable capacitance is connected across the stator winding of an induction machine and self-excitation occur under favorable conditions. SEIG is good candidate for electric generation applications, because they do not need external power supply to produce the magnetic field. According to D. Seyoum et al. (2000) permanent magnet generator can also be used for energy applications but they suffer from uncontrollable magnetic field, which decays over a period due to weakening of the magnets, and generated voltage tends to fall steeply with load.

The advantages of SEIG over synchronous induction machine are small size and weight, simple construction, absence of separate source for excitation, cheap and low maintenance cost. Besides its application as a generator, the principle of self-excitation can also be used in dynamic braking of three phase induction motor. The terminal capacitance in SEIG must have a certain minimum value so that the self-excitation may take place. This value is affected by the machine parameters, its speed and load condition (A.K. Tandon et al., 1984 and Malik et al., 1987).

2.3 POWER LOSS

The energy efficiency is an important parameter to a FESS. The total efficiency of a FESS depends on the power losses. Flywheel must be rotating continuously overcoming its mechanical loss, P_{loss}, which consist of an axial rotating loss, P_{ax}, windage loss, P_{wind}, copper loss, P_{cu} and iron core loss, P_{Fe}. The power losses of the system can be calculated by equation;

$$P_{loss} = P_{ax} + P_{wind} + P_{cu} + P_{Fe} \tag{2.7}$$

To improve the efficiency of a FESS, the windage loss must be reducing. This is because the windage loss is the largest amount of losing from the total losses. Then, generally a vacuum enclosure used to reduce the mechanical losses.

On the other hand, using helium-air mixture gas is a better way to reduce the windage loss. Of course, using this kind of technologies can improve the total efficiency of the system (Liu, H., and Jiang, J.,2007).

2.4 ELECTRICAL SWITCH

Switch is an electrical component that can break an electrical circuit, interrupting the current or diverting it from on conductor to another (Falex., 2008 and Houghton Mifflin., 1979). Switch can be classified to two types; manually operated switches and automatically operated switches.

2.4.1 Single Pole Double Throw (SPDT) Relay

SPDT relay is an electrical switch that automatically manipulated by signal. Many relays use an electromagnet to operate a switching mechanism mechanically, but other operating principles are also used. Generally, relay switches are used to control a high-voltage circuit with a low-voltage signal, as in some types of modems or audio amplifiers and to control a high-current circuit with a low-current signal, as in the starter solenoid of an automobile and etc.

2.5 COMPUTER-AIDED DESIGN AND COMPUTER-AIDED MANUFACTURING (CAD/CAM)

Computer-aided design and computer-aided manufacturing (CAD/CAM) are a computer system which is used to both design and manufacture products. CAD used to create the computer models which defined by geometrical parameters. But, CAD/CAM systems are used both for designing a product and for controlling manufacturing process. The geometries in the CAD drawing are used by the CAM portion of the program to control a machine that creates the exact shape that was drawn. CAD/CAM software is most often used for product development, machine-tooling and manufacturing.

The developments in solid modeling systems bring an enhanced environment for generation NC tool path. The CAD/CAM used to generate G-code for making automatic generation of the tool path in NC machining (You et al., 1995). G-code is common name which used for numerical control (NC) programming language. G-code generated from CAD/CAM mainly used in automation of machining process. The G-code gives instruction to the cutting tool to move. The machining process from stock material to the finished part include various different stages, including rough cut, semi-finish cut, and finish cut. Every stage might have a number of sub-machining processes (You et al., 1995).

2.6 MACHINING

Machining is a material removal process in which a sharp cutting tool is used to mechanically cut away material so that the desired part geometry remains. Machining processes are classified as turning, milling and drilling. Other machining operations such as shaping, planning, boring, broaching and sawing are falling into miscellaneous operations.

2.6.1 Turning

Turning is a single point cutting tool removes material from a rotating workpiece to generate a cylindrical shape. Machine tool that used in turning process is

n a lathe are facing, counter turning,

occur on both external and internal

ɔured part. Parts ranging from pocket

ller shafts can be turned on a lathe.

the cutting tool rotates to bring cutting

operations are performed on milling

ess in industry for machining parts to

ɹn about an axis while a workpiece is

of the cutter are able to shave chips of

ed based on the spindle position. The

:tical position. Milling processes are

.ual cuts on the material in a single run;

many teeth, spinning the cutter at high

cutter slowly. Most often it is some

'wiki/Milling_%28machining%29).

2.6.3 Drilling

Drilling is a cutting process that enlarges a hole of circular cross-section in solid material by using drill bit. The drill bit is a rotary cutting tool, often multipoint. The bit is pressed against the workpiece and rotated at rates from hundreds to thousands of revolutions per minute. This forces the cutting edge against the workpiece, cutting off chips from what will become the hole being drilled (http://en.wikipedia.org/wiki/ Drilling).

2.7 CONCLUSION

In this chapter, extracts from previous studies and reports were extracted and cited in order to improve understanding on variables involved in this study. FESS is a system that can generate a backup power to a critical load. The energy stored in the flywheel rotor depends on the shape and properties of the material.

CHAPTER 3

RESEARCH METHODOLOGHY

3.1 INTRODUCTION

In this chapter, the methods and techniques used to conduct this research are deliberated step by step. Methodology is an important part where it precisely describes and discusses the methods to achieve and accomplish the objectives of this research. This chapter consists of three sections. Firstly, prepared a suitable raw material for flywheel rotor and experiment bench, and fabricate it based on design. Then, a power electronic circuit to control the motor-generator set and generator circuit were constructed. Finally, the flywheel rotor and power electronic switch were installed to the induction machine and data was taken from the experiment.

3.2 FLYWHEEL ROTOR AND EXPERIMENT BENCH OF FESS

Here, this study consists of two main raw materials as aluminium alloy block for flywheel rotor and stainless steel for experiment bench. The raw materials undergo some machining operation to fabricate.

3.2.1 Materials

Table 3.1: Material used to fabricate flywheel rotor and experiment bench

Raw material	Grade	Uses
Aluminium alloy (350x350x35)mm	1000 series	Aluminium alloys are widely used in engineering structures. Aluminium is the most widely used non-ferrous metal. Other than that, aluminum used worldwide as a material for automotives, heat sink, construction and other engineering applications.
Stainless Steel (650x550x5)mm	ASI 304	There are over 150 grades of stainless steel, of which fifteen are most commonly used. Generally stainless steels milled into coils, sheets, plates, bars, wire, and tubing to be used in cookware, cutlery, household hardware, surgical instruments, industrial equipment and as an automotive and aerospace structural alloy and construction material in large buildings.

3.2.2 Equipments

Equipments that used to fabricate flywheel and experiment bench are:

i. Milling machine
ii. Lathe machine
iii. Welding
iv. Shear machine
v. Bending machine

3.2.3 Design of Flywheel

In this study, the shape that chosen for the flywheel is thin firm and the shape factor is about 0.5. The diameter and thickness of the flywheel rotor are 340 mm and 25 mm respectively. This design consists of an island on front side and a key shaped hole on another side of the flywheel rotor. Here, the purpose of the island is to support the flywheel from moving away. On the other side of flywheel rotor, a key shape was pocketed about 20 mm. This key shape was designed purposely to lock the flywheel with the motor rotor. The design of flywheel rotor that drawn in CATIA is shown in figures 3.1 and 3.2 respectively (*detail technical drawing of flywheel rotor is shown in Appendix C.1). The flowchart of this part is shown in figure 3.4.

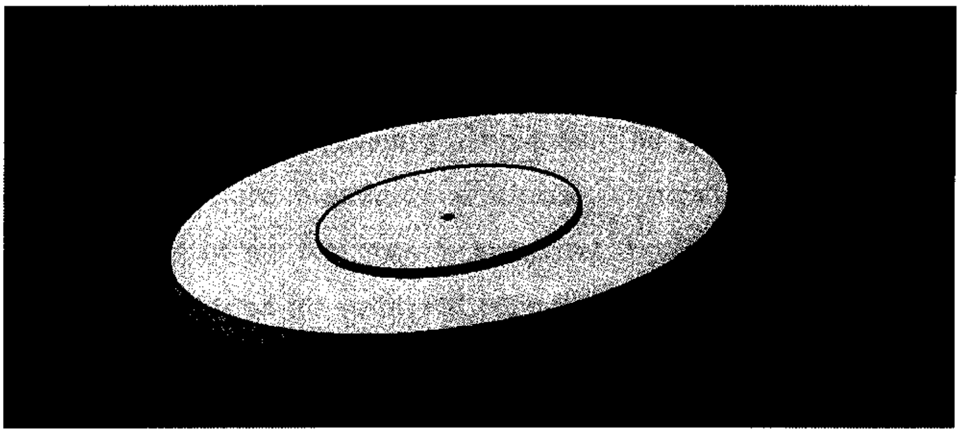

Figure 3.1: Top view of flywheel rotor

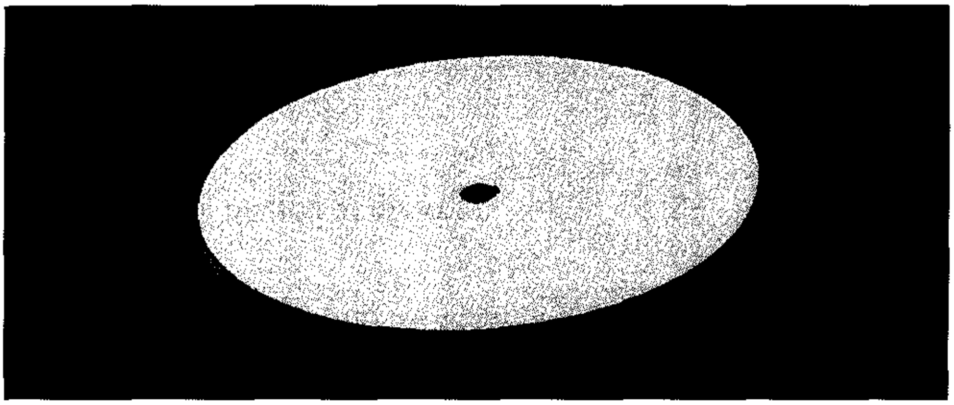

Figure 3.2: Bottom view of flywheel rotor

3.2.4 CAD/CAM

In this study, the tool that used to design the flywheel rotor is CATIA. This design was drawn including machining simulation. The G-code was generated from CATIA at the end of the machining simulation. Generally, the G-code used for automatic generation of the tool path in numerical controlled machining. G-code is common name which used for numerical control (NC) programming language (*the generated G-code is shown in Appendix D).

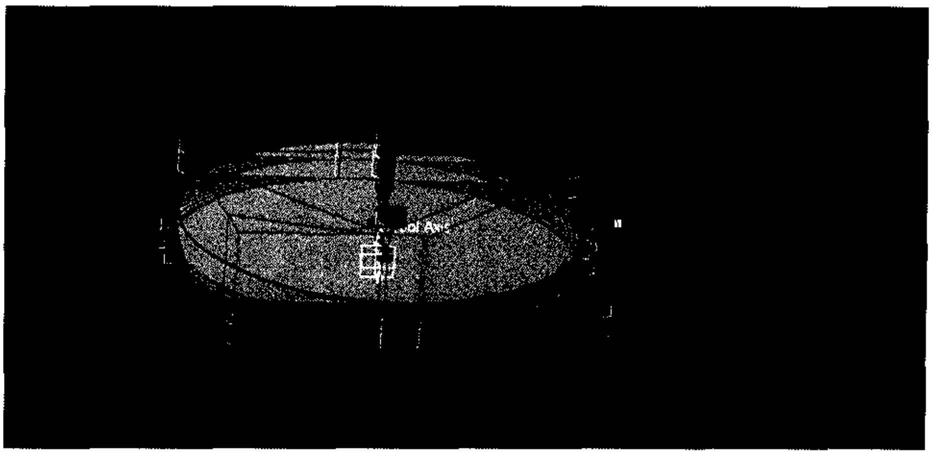

Figure 3.3: Machining simulation in CATIA

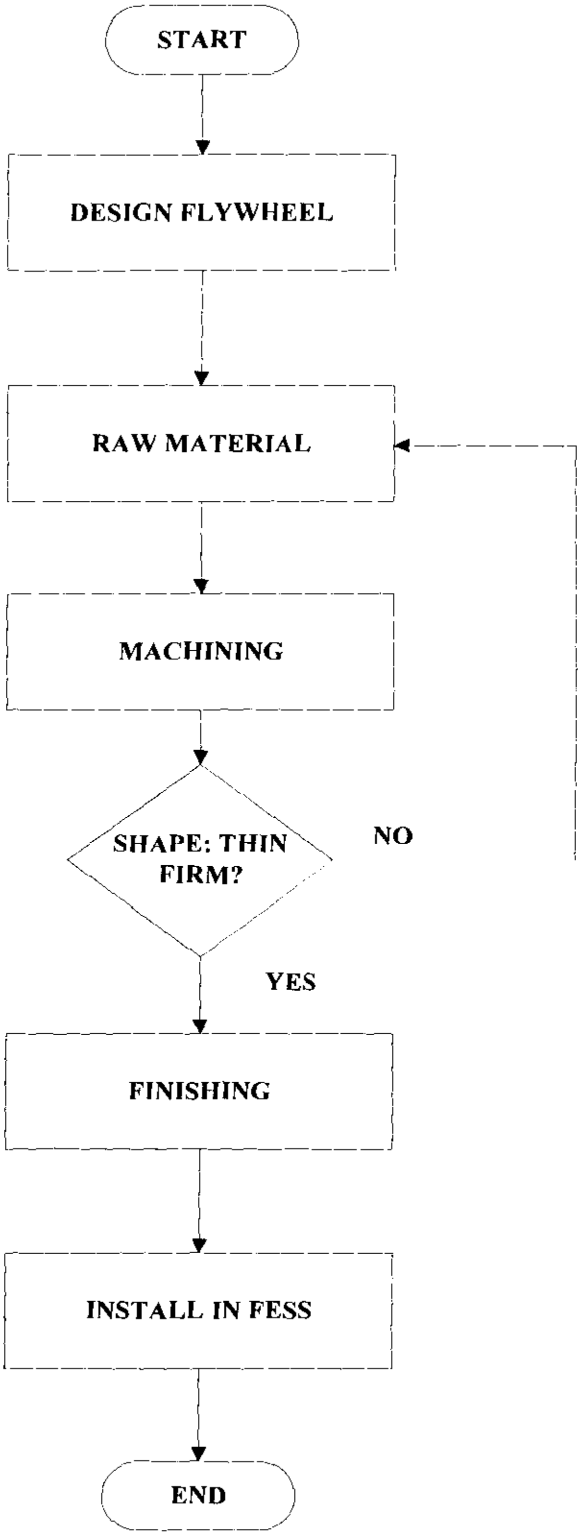

Figure 3.4: Flowchart for mechanical part

3.2.5 Machining operation of flywheel rotor

The size work piece that prepared for flywheel is 350 x 350 x 35 mm. Here, the automatic tool generation cannot be conduct at laboratory because the work piece is dimensionally too large. So, the flywheel was fabricated manually by milling machine and lathe machine.

3.2.5.1 Milling operation

Firstly, the raw material was clamped directly in the milling machine. The raw material was pocketed up to 20mm depth by using 10mm end mill. Then, a hole was drilled to get the key shape. After drilled, the raw material was unclamped and it was filed to remove the burrs. The direct clamp of raw material and pocketing processes are shown in figures 3.5 and 3.6 respectively.

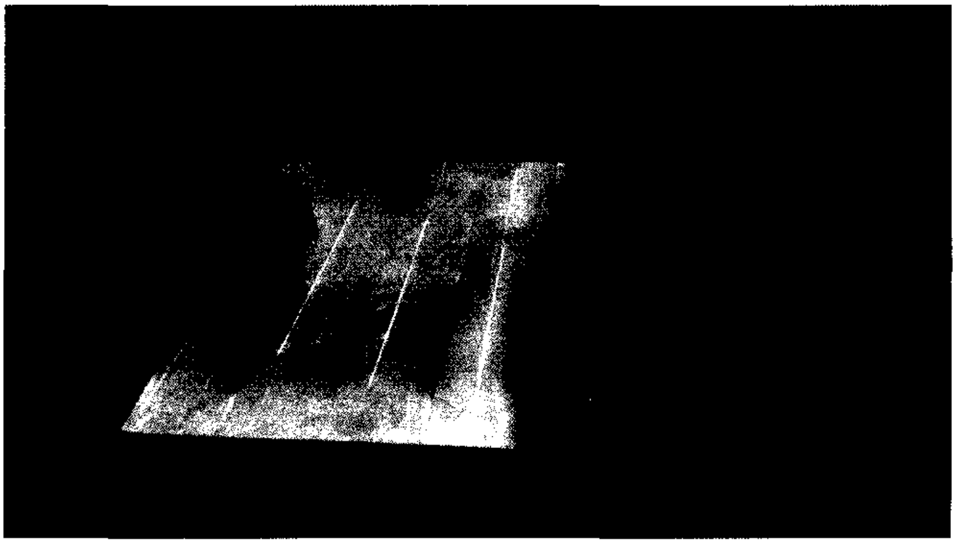

Figure 3.5: Raw material was clamped directly in milling machine

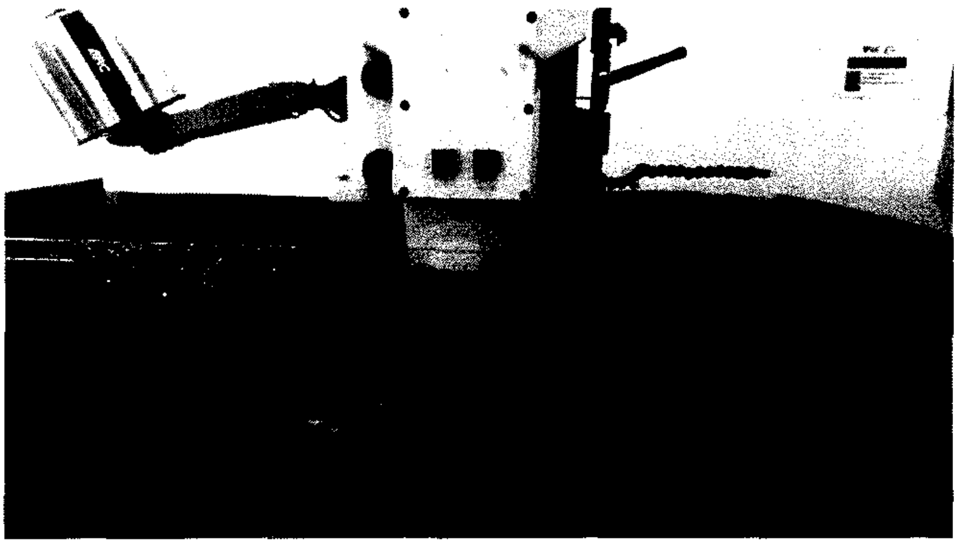

Figure 3.6: Pocketing process on raw material

3.2.5.2 Lathe operation

Here the lathe used to reduce the diameter of a part to a desired dimension. After milling process, the raw material was clamped securely in the lathe chuck to undergo a turning process. Then, install a roughing or finishing tool. Move the tool off the part by backing the carriage up with the carriage hand wheel, and then use the cross feed to set the desired depth of cut. The clamped material was cut into cylindrical shape by turning operation. The diameter of the flywheel rotor is 170mm and the thickness is 25mm. After the material cut into cylindrical shape, an island was cut. The diameter of island is 160mm and thickness of 5mm. Finally, the flywheel rotor undergoes profile finishing turning operation to remove the sharp edges. The flywheel rotor that fabricated is shown in figure 3.7. (*parameters and calculation of flywheel rotor are shown in Appendix A.1)

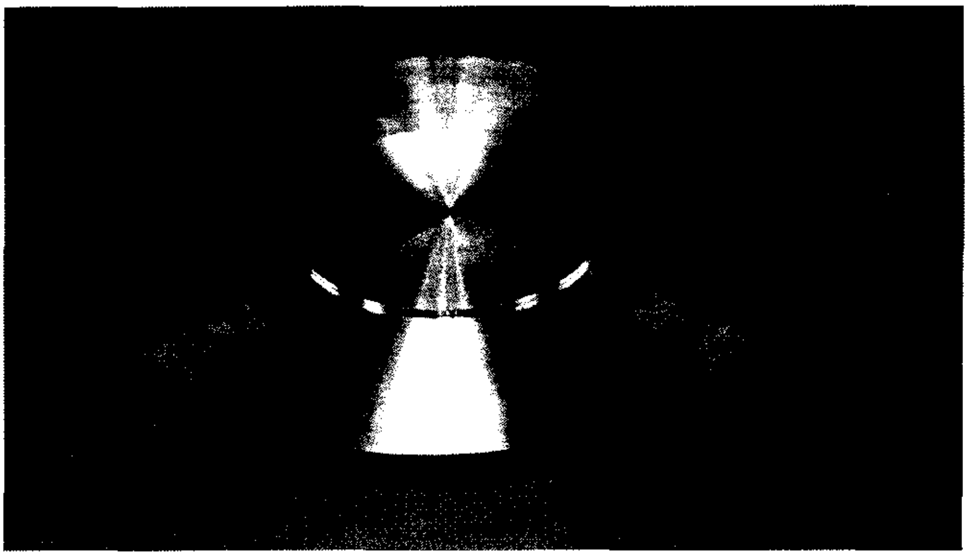

Figure 3.7: Flywheel rotor

3.2.6 Experiment Bench

The experiment bench was made by stainless steel with dimension of 650 mm x 550 x 5 mm. Firstly, cut the metal sheet by using shear machine. Then, it was drilled and pocketed (through hole) by milling machine. Finally, the legs of bench were welded (*the complete mechanical parts are shown in Appendix E.1)

3.3 ELECTRICAL PART

There are two types of circuit was used in this study. Firstly, the power transfer switches circuit. Secondly, generator circuits for three different capacitance which are 33μF, 47μF and 68μF (N.H. Malik and A.A. Mazi, 1987 and Swathi devabhaktuni and S.V.Jayaram kumar, 1998). The electronic components that used for this study is shown in table 3.2.

Table 3.2: Electronic components

Components	Unit
15V Step down transformer	1
Voltage regulator, L7809CV	2
Diode, 1N4003	6
Capacitor, 220μF 50V	2
Capacitor, 10μF 50V	2
Heat Sink	2
Resistor, 18Ω	2
Capacitor, 33μF 350V	3
Capacitor, 47μF 350V	3
Capacitor, 68μF 350V	3
SPDT relay	6
Fuse holder	2
Fuse, 15A	1
Fuse, 1.5A	1
3 phase circuit breaker	1

(*datasheet of components are shown in Appendix F)

3.3.1 Power Transfer Circuit

In this study, a circuit that produced 9V signal was designed as shown in figure 3.8. Here, the 9V signal used to activate SPDT relay switch. The SPDT relay switches were used to control the FESS automatically. Then, the signal of this circuit was tested by oscilloscope before it connects to the SPDT relay switch (*the result of signal circuit is shown Appendix F.5)

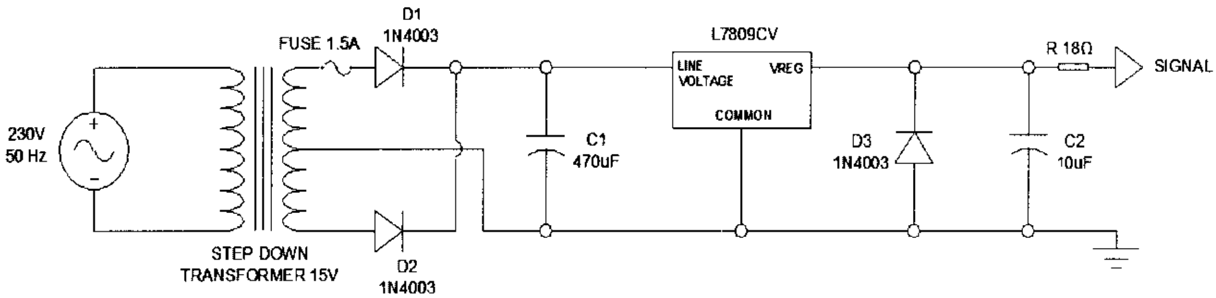

Figure 3.8: Signal circuit

3.3.2 Design of Excitation Capacitance for Self-Excited Induction Generator (SEIG)

A 3 phase asynchronous induction machine was connected in wye (Y) connection as shown in figure 3.9. In wye (Y) the stator windings are connected from phases of the supply to the neutral. Then, to generate the power, it was applied SEIG technique. The capacitors are connected across every stator terminal as shown n figure 3.10.

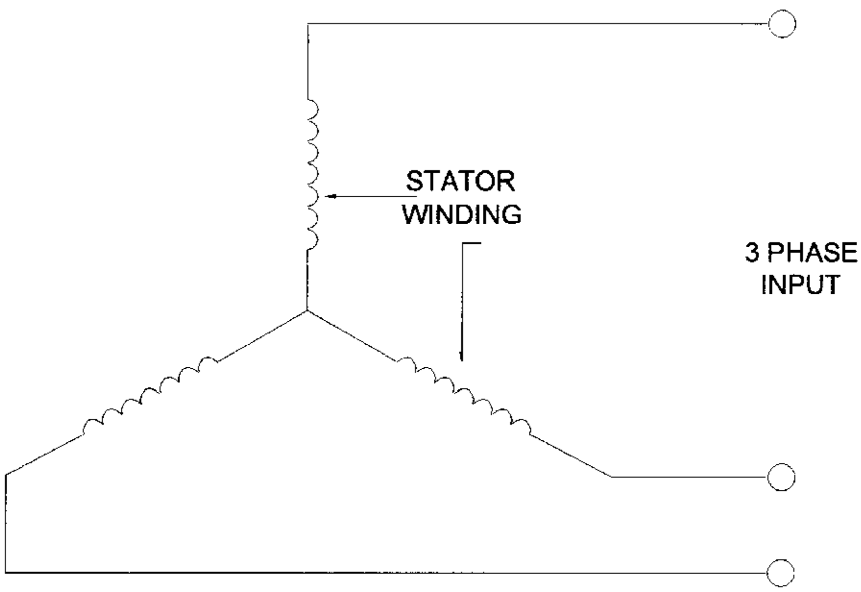

Figure 3.9: Wye (Y) connection for 3 phase induction machine

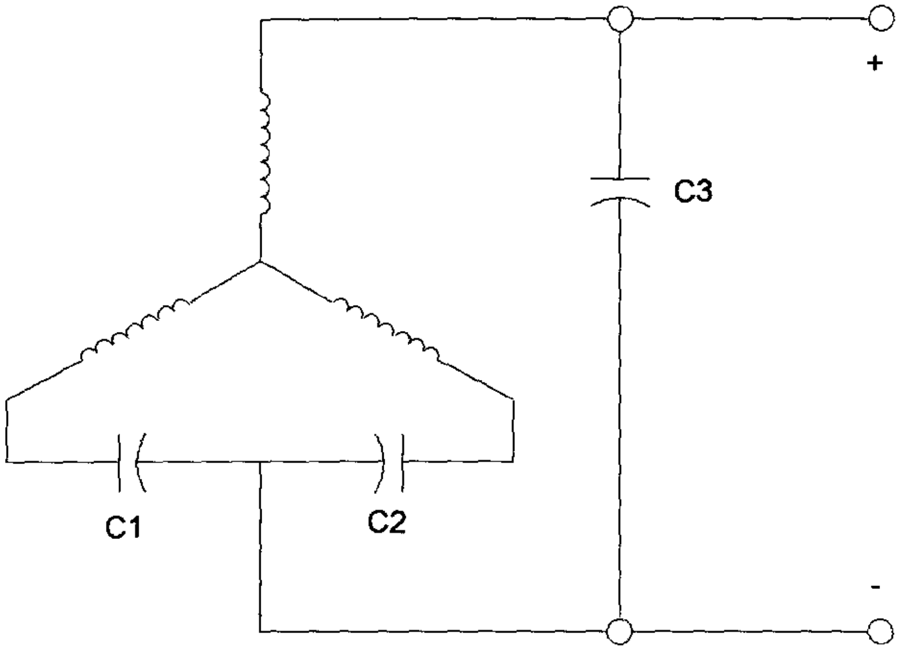

Figure 3.10: Generator circuit

3.4 EXPERIMENT OF FESS

Before the experiments started, the flywheel rotor assembled to the rotor of induction motor. Firstly, the induction machine was placed on the experiment bench. A L shape holder used to attach both experiment bench and the induction machine. M8 bolts and nuts were used to tight the induction machine to the experiment bench. Then, the flywheel rotor installed to the rotor of the induction machine by using M6 stainless steel bolt (*bolts and nuts that have been used to assemble the FESS are shown in Appendix G.1) and the system that drawn in CATIA is shown in figure 3.11. A rubber washer was placed into the flywheel rotor to reduce the frictions between flywheel and rotor of induction machine. After that, stator terminals of induction machine connected to the three phase power and also to generator circuit. The FESS that assembled is shown in figure 3.12.

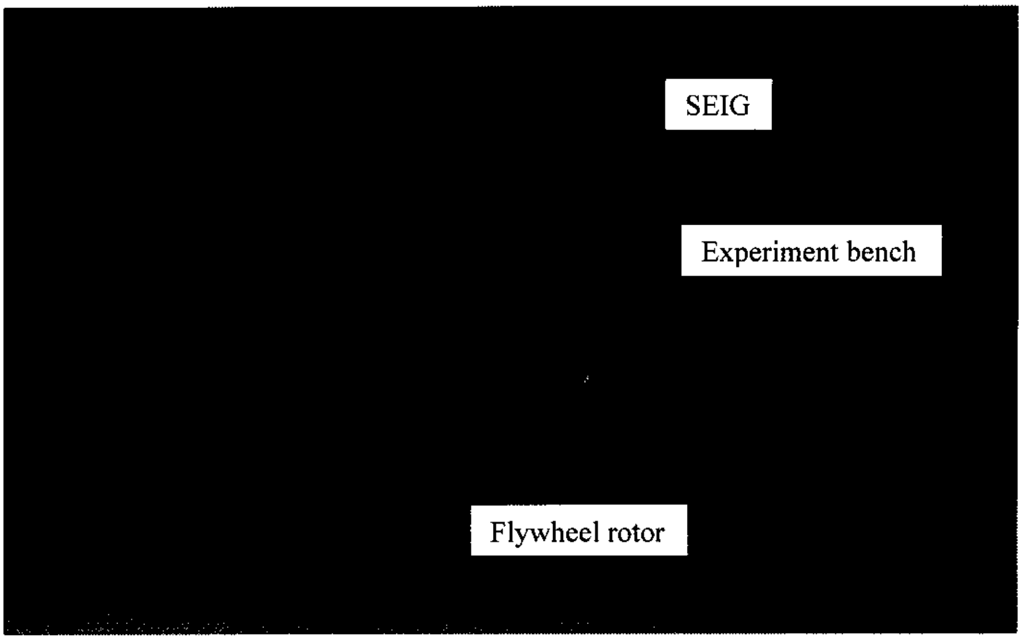

Figure 3.11: Isometric view of FESS

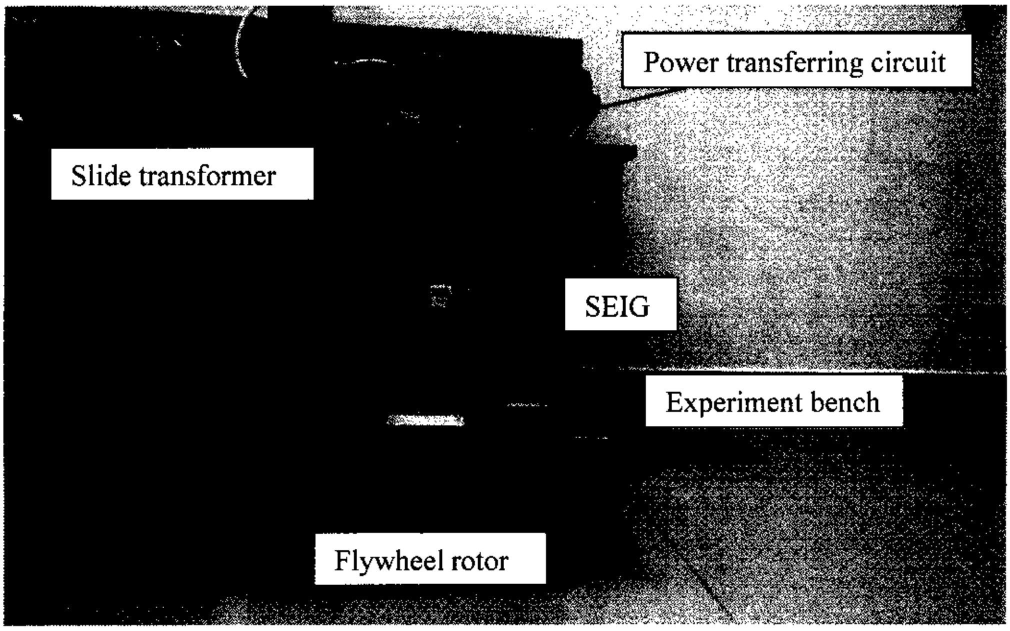

Figure 3.12: FESS after assembled

Figure 3.13 and 3.14 shows, the block diagram and flowchart of FESS respectively. The process flow the system begins with produce 9V signal from the signal circuit. When a 9V signal received by the power exchange unit, the SPDT relays (normally open) open the gate. So, the motor generator set acts as motor and the flywheel start to rotate. The voltage increased slowly by using phase indicator. On the other side, the SPDT relays at load circuit (normally open) open the gate to the load. When there is a blackout occurs, the motor-generator set acts as a generator. The SPDT relays at generator circuit (normally closed) open the gates while the gates at load circuit and motor circuit are closed. The voltage generated supplied to the critical load through the relay.

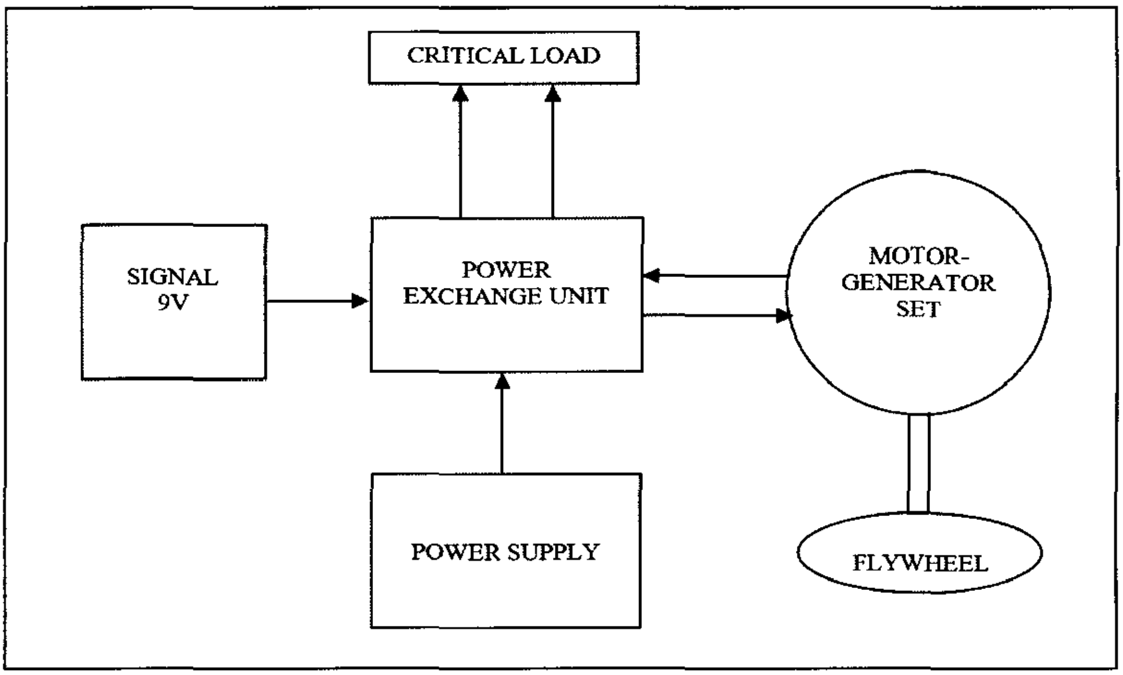

Figure 3.13: Block diagram of FESS

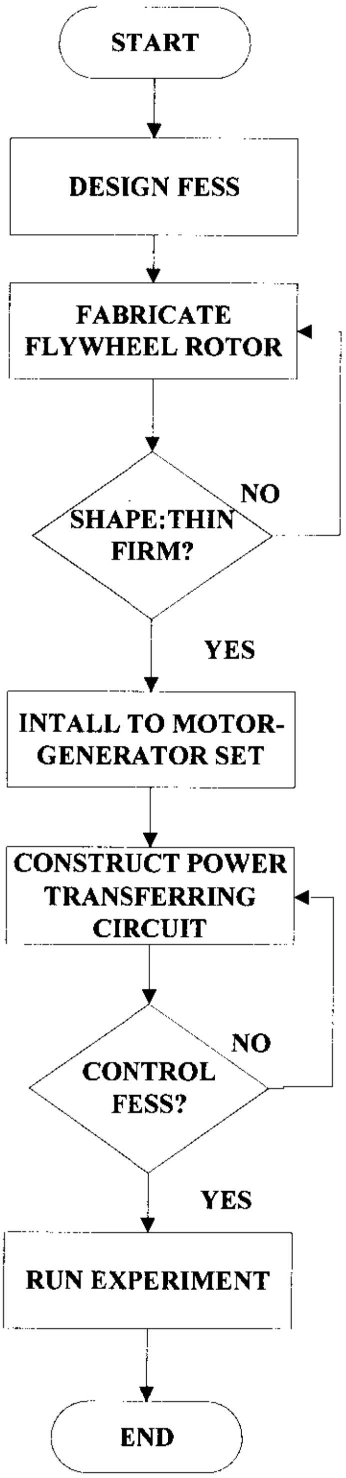

Figure 3.14: Flowchart of FESS

3.4.1 Equipments

Equipments that used to fabricate flywheel and experiment bench are:

I. Oscilloscope
II. Multimeter
III. Photo contact tachometer
IV. Slide transformer

3.4.2 Experiment 1: Motor-generator set as motor

In this experiment, induction machine was used as a motor. Firstly, the three phase voltage increased slowly up to 415 V and the speed of the flywheel rotor was recorded for every 50 V. The speed of flywheel rotor was recorded in revolution per minute (rpm) by using photo contact tachometer as shown in figure 3.15. Here, the slide transformer was used to increase the voltage. After the flywheel rotor achieved a constant speed, the three phase power was switched off. Then, the rotation time of flywheel rotor and the rpm of the rotor were recorded. The experiment was repeated for three times and an average value was calculated. Finally, the graphs of rpm versus voltage and rpm versus time (ds) were plotted respectively.

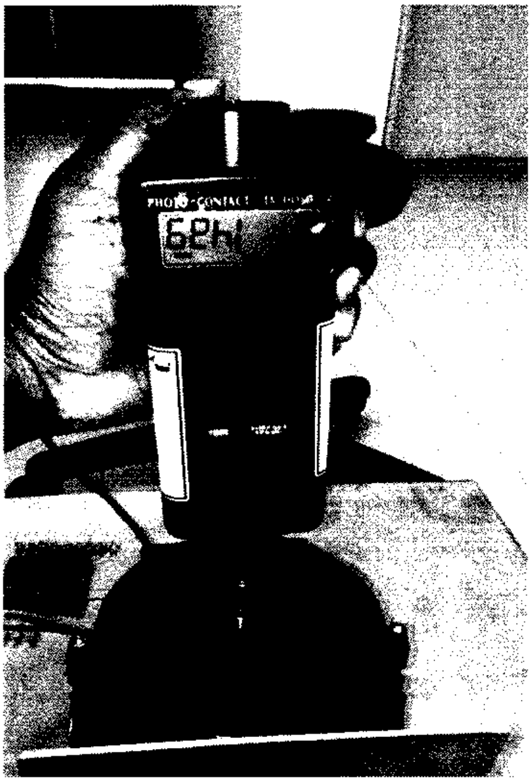

Figure 3.15: Photo contact tachometer

3.4.3 Experiment 2: Motor-generator set as generator

In this experiment, the motor-generator set was acting as generator. Firstly, make sure that the stator terminals of induction machine were connected to the generator capacitance circuit for 33μF. The three phase power source supplied to the motor-generator set. When it achieved a constant speed at 415 V, main power was switched off. Then, the voltage that generated was recorded. A multimeter and stopwatch are used to record the data. Then, the experiment was repeated for three times and an average value was calculated. The graphs of voltage against time (ds) and voltage versus rpm were plotted respectively. These steps were repeated for 47μF and 68μF (*pictures that were taken during experiment are shown in Appendix I).

CHAPTER 4

RESULTS AND DISCUSSIONS

4.1 INTRODUCTION

This chapter mainly summarizes all tabulated data from the study findings. Later in this chapter, detailed justifications are available on the generated voltage at different capacitance and comparison between motor and generator mode.

4.2 MOTOR-GENERATOR SET OF FESS AS MOTOR

4.2.1 The speed of flywheel rotor when the input voltage increases

Table 4.1 shows that, the speed (rpm) of the flywheel rotor varies with the input voltage. This experiment started by increasing of the input voltage. Here, the average speed was taken to reduce the error. The input voltage has to increase slowly, because in an induction machine, stator is powered by alternating current (ac) and designed to rotate in time with AC oscillations as rotating magnetic field present. Furthermore, to start an induction motor, initially high starting current is needed, before it is stable. The, a high rate of magnetic torque present initially before stabilize, that is due to motor that reaches its maximum torque, at about 20% or 0.02 of slip.

Besides that, the rotor speed becomes unstable during startup and it is being control by the number of pole pairs and frequency of supply voltage. Rotor speed turns stable as the shaft rotation speed is kept above the peak torque point. It also can be said, the speed of rotor will be constant after a peak torque point. Besides that, in an induction motor, the slip or speed at which the maximum torque occurs can be controlled by varying the rotor resistance. The value of that maximum torque is independent of the rotor resistance. A high rotor resistance lowers the speed at which maximum torque occurs and thus increases the starting torque of the motor. So, sudden start of an induction machine might cause the rotor to damage. The parameters of induction motor and characteristics (MATLAB Simulink) of the induction machine are shown in Appendix A.2 and B respectively)

Table 4.1: Speed (rpm) of flywheel rotor at different input voltage

Voltage, V	Revolution per minute, rpm			
	1st reading	2nd reading	3rd reading	Average
0	0	0	0	0
50	600	625	650	625
100	1194	1200	1225	1206
150	1470	1390	1471	1444
200	1480	1479	1481	1480
250	1489	1485	1487	1487
300	1492	1491	1495	1493
350	1495	1494	1495	1495
400	1497	1497	1497	1497

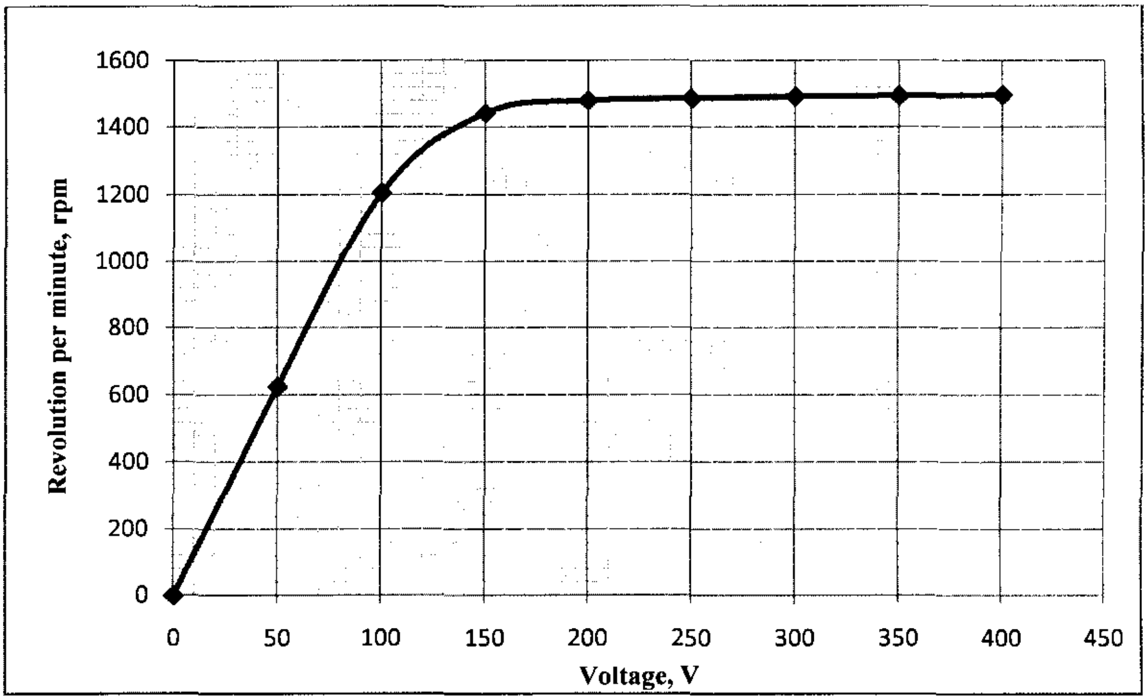

Figure 4.1: Graph of revolution per minute (rpm) versus voltage (V)

Figure 4.1 shows that, the graph of revolution per minute (rpm) versus voltage (V). The trend of the graph shows that, the speed (rpm) of flywheel rotor increased rapidly and it achieved a constant state at end of the experiment. At 50V the speed of flywheel rotor is 625rpm. Then, it was increasing rapidly to1206 rpm at 100V. After 150V, the speed of the flywheel rotor increased slowly until it achieved a constant speed of 1497 rpm at 400V. From the graph, it can be said that, the rotor rotate up to rated speed (1497 rpm) which near to the synchronous speed of motor (1500 rpm).

4.2.2 The free rotation of flywheel rotor, when the power shut down

Table 4.2 indicates that, time taken to rotate by flywheel rotor when the power shut down. For this experiment, the power was shut down when the flywheel rotor achieved rated speed. Then, the speed (rpm) of flywheel rotor was recorded for every 10 seconds.

Table 4.2: Time taken to rotate by flywheel rotor when the power shut down

Time, s	Revolution per minute, rpm			
	1st reading	**2nd reading**	**3rd reading**	**Average**
0	1497	1497	1497	1497
10	1182	1198	1196	1192
20	967	955	961	961
30	735	740	745	740
40	531	535	539	535
50	331	332	342	335
60	149	141	142	144
70	25	28	27	26.67
80	0	0	0	0

Figure 4.2 shows that, graph of revolution per minutes (rpm) against time (s). The trend of graph indicates the speed (rpm) of the flywheel rotor decreases with the time (s). At 0s the speed of the flywheel rotor is about 1497 rpm. At 30s the speed (rpm) of the flywheel rotor is almost half of the rated speed, 740 rpm. The speed (rpm) of the flywheel rotor decreases slowly and it achieved 0 rpm at 80s. The duration of flywheel rotor to rotate depends on the properties of material and also moment of inertia of flywheel rotor. The moment of inertia of flywheel rotor that was used in this study is 0.075 kg.m^2, while the moment of inertia of rotor motor is 0.016 kg.m^2. When the moment of inertia of flywheel rotor is high than rotor motor, the flywheel rotor will able to rotate more time (*the parameter and calculation for moment of inertia of flywheel rotor are shown in Appendix A.1).

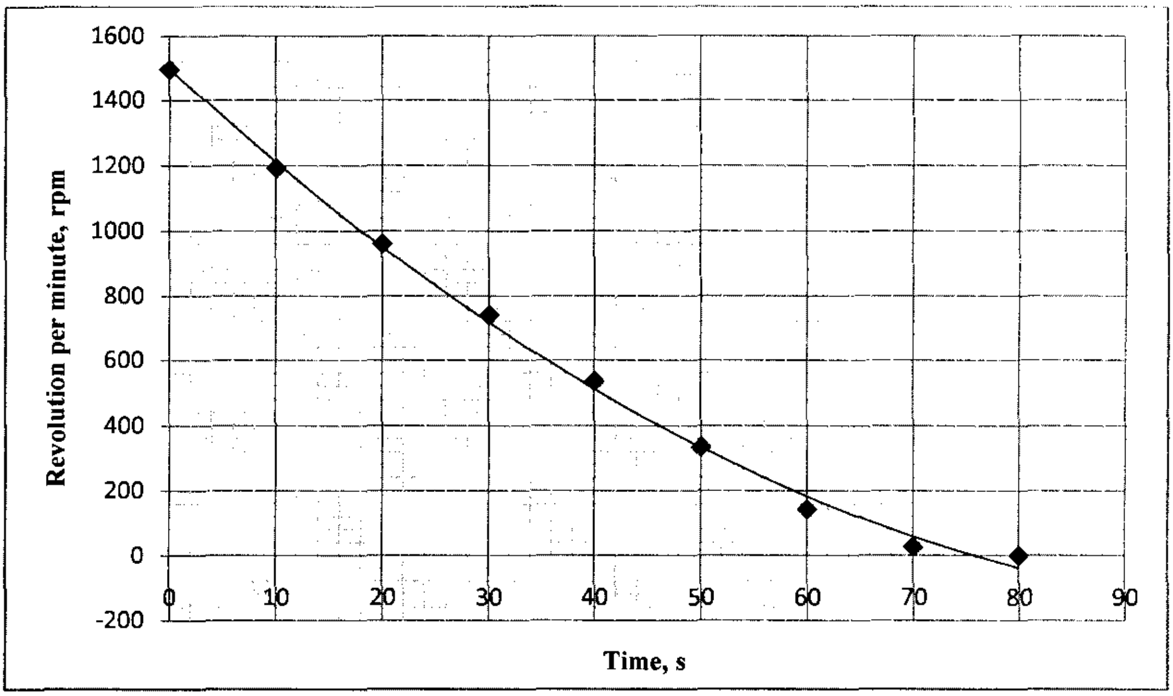

Figure 4.2: Graph of revolution per minutes (rpm) versus time (s)

4.3 MOTOR-GENERATOR SET AS GENERATOR

For this experiment, the theory of SEIG applied to the induction machine for three different values of capacitors (33μF, 47μF and 68μF). For all three cases, the generated voltage with time (ds) was recorded. Then, the drop of voltage with speed (rpm) of flywheel rotor will discuss.

4.3.1 Case 1: 33μF

Table 4.3 shows the voltage that generated by FESS when the power was shut down. From the table, it can be said that FESS generated voltage for a very short period.

Here, the period of generated voltage measured in deciseconds (ds) and the voltage was recorded by using multimeter as shown in figure 4.3.

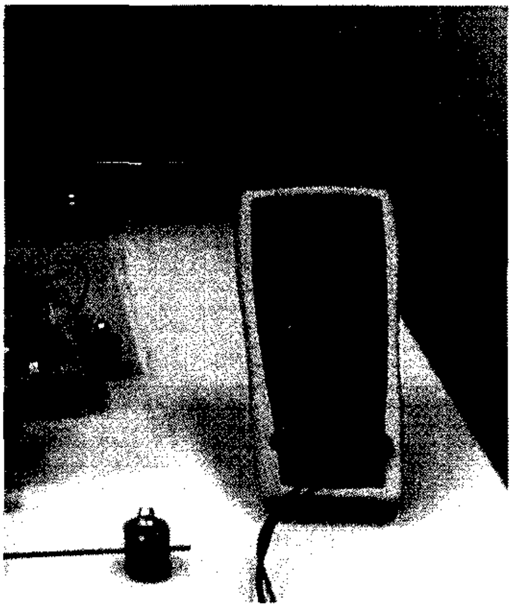

Figure 4.3: Generated voltage for 33μF is shown in multimeter

Table 4.3: Generated voltage when power shut down (33μF)

Time, ds	Voltage, V			
	1st reading	**2nd reading**	**3rd reading**	**Average**
0	214.3	224	211.6	215.63
5	164	163	160.3	162.43
10	126.1	125	127.1	126.07
15	94	90	89	91
20	62.4	63	61	62.13
25	38	35	33.6	35.53
30	12	18	16	15.33
35	0.56	0.3	0.12	0.33

Figure 4.4 indicates the graph of voltage (V) versus time (ds). The trend of the graph shows the voltage decreases uniformly with the time (ds). For 33µF, FESS able to generate up to 216V instantly when the blackout occurs. At 15 ds and 20 ds the voltage decreases to 91V and 62V respectively. The voltage becomes 0.33V which is almost to zero at 35 ds.

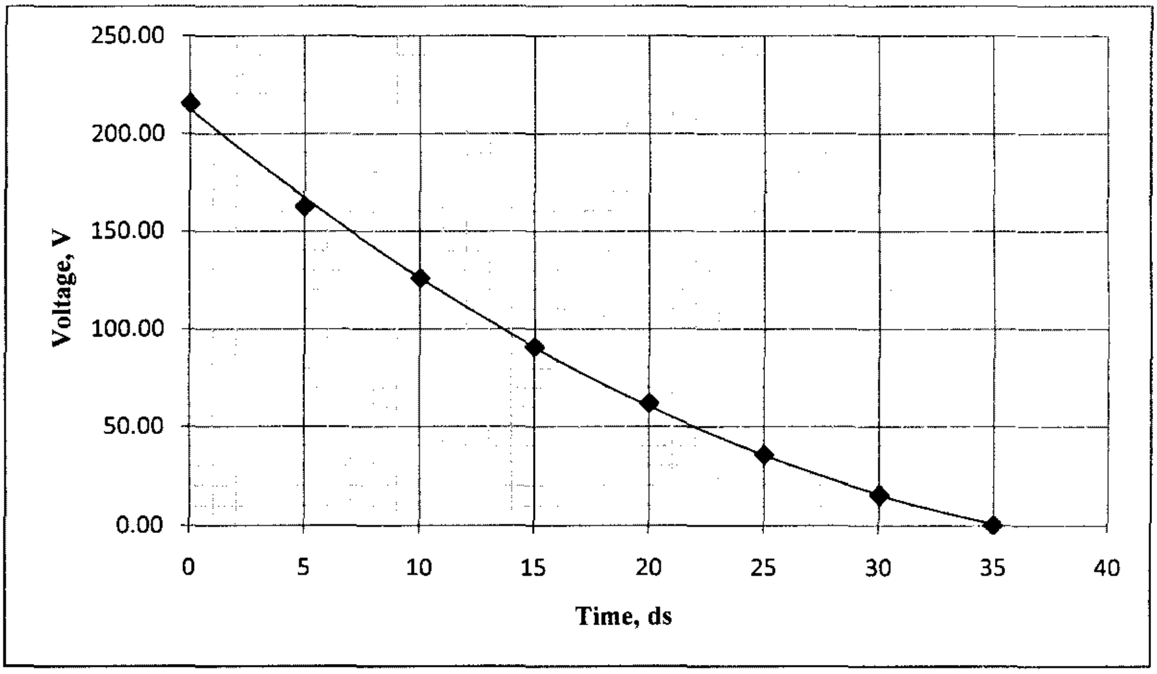

Figure 4.4: Graph of voltage (V) versus time (ds) for 33µF

Table 4.4 shows the drop of the voltage with speed of the flywheel rotor. From this table, it can be said that, the voltage decreases rapidly with decreases of the speed of the flywheel rotor. From this table, a graph of voltage (V) versus revolution per minute (rpm) was plotted as shown in figure 4.5. According to the graph, the voltage generated by FESS is high at rated speed. When the speed of flywheel rotor decreases, the voltage also decreases. According to the graph, the FESS generated 217.4V when the rotor rotated near to the rated speed about 1496.33 rpm. When the flywheel rotor rotated at 1128 rpm, the motor-generator set able to generate 78V. At the speed of 833.3 rpm the voltage decreases to 1.1V and becomes inconsistence.

Table 4.4: The voltage drop with speed of flywheel rotor (33μF)

Voltage, V				Revolution per minute, rpm			
1st reading	2nd reading	3rd reading	Average	1st reading	2nd reading	3rd reading	Average
214.3	221.3	216.6	217.40	1496	1497	1496	1496.33
165	163.2	162	163.4	1389	1391	1402	1394.00
121.3	121.3	108.3	118.3	1348	1356	1341	1348.33
77	76.5	81.6	78.37	1131	1121	1132	1128.00
61.8	59.6	62	61.13	942.3	931	962.1	945.13
35.4	37.9	30.1	38.30	908	887.3	886	893.77
12.3	18.3	14.7	15.10	867	852	868	862.33
1	1.4	0.9	1.1	842	831	827	833.33

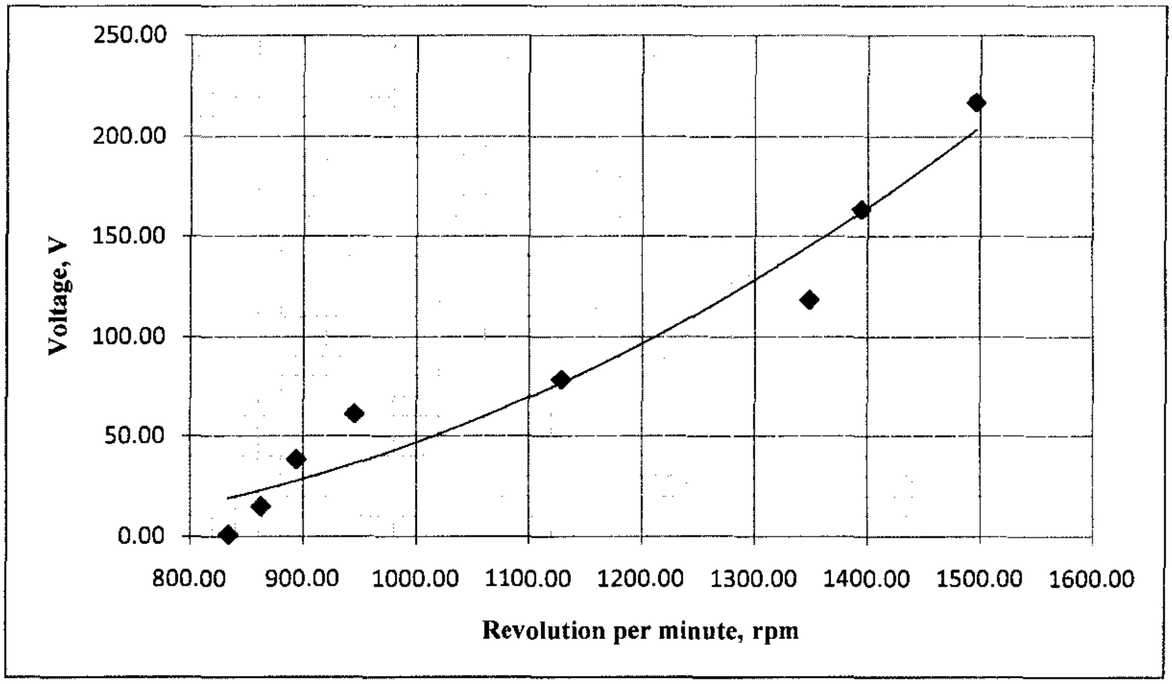

Figure 4.5: Graph of voltage (V) versus revolution per minute (rpm) for 33μF

4.3.2 Case 2: 47μF

In this, experiment, the capacitors of 33μF in SEIG are replaced to 47μF. Table 4.5 shows, the voltage that generated by FESS for a short period. A graph of voltage (V) versus time (ds) was plotted based on table 4.5.

Table 4.5: Voltage that generated by FESS for a short period (47μF)

Time, ds	Voltage, V			
	1^{st} reading	2^{nd} reading	3^{rd} reading	Average
0	236.5	232.4	228.9	232.60
5	131.9	132.5	130.4	131.60
10	115.2	112.5	109.6	112.43
15	83.1	80.1	81.9	81.7
20	53.6	52.9	52.1	52.87
25	39.1	32.6	35.7	35.80
30	12.9	15.1	13.5	13.83
35	0.9	1.2	1.1	1.07

The trend of the graph in figure 4.6 is almost same with the graph in figure 4.4. In this case, the FESS generated about 232.6V instantly when the main source was shut down. Then, the generated voltage decreased very rapidly in few deciseconds. At 15 ds, the voltage decreased to 81.7V and it becomes to 1.07V at 35 ds. When compared to case 1, the FESS more voltage for this case. This is because; 47μF might be a suitable minimum value of capacitance for SEIG.

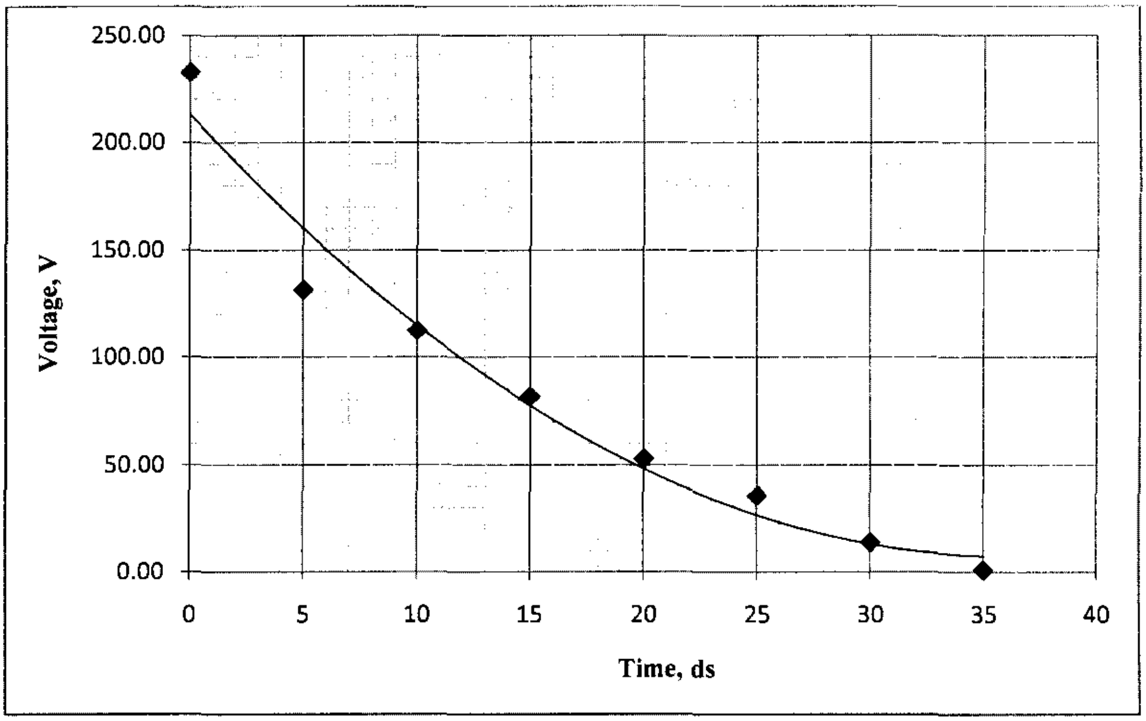

Figure 4.6: Graph of voltage (V) versus time (ds) for 47μF

Table 4.6 shows, the drop of voltage generated by FESS with speed (rpm) of flywheel rotor. From this table, a graph of voltage (V) versus revolution per minute (rpm) was plotted as shown in figure 4.7. For this case, the FESS able to generated up to 232V at the speed of 1495 rpm. When, the flywheel rotor rotated at 1108 rpm, the FESS still able to generate 71.3V. The voltage level at the speed of 912 rpm and 850 rpm are 39.9V and 11.6V respectively. Then, the voltage decreased to 0.43V at 815.1 rpm and it becomes inconsistent of voltage for rest of rotation.

Table 4.6: The drop of voltage with speed of the flywheel rotor (47μF)

Voltage, V				Revolution per minute, rpm			
1st reading	2nd reading	3rd reading	Average	1st reading	2nd reading	3rd reading	Average
236	232.6	228.4	232.33	1497	1496	1493	1495.33
132.6	136.5	139.2	136.1	1352	1348	1341	1347.00
115.5	112.3	113	113.6	1212	1219.6	1220	1217.20
98.9	95.2	91.3	95.13	1164	1159	1161	1161.33
71.3	69.9	78.6	73.27	1114	1109	1102.3	1108.43
39.9	38.7	35.8	38.13	912	908	917	912.33
22.6	19.6	19.1	20.43	871	872	869	870.67
11.6	11.7	11.1	11.47	850	851	849	850.00
6.2	5.9	5.8	5.97	831	834.2	832	832.40
0.3	0.9	0.1	0.43	819	812.3	814	815.10

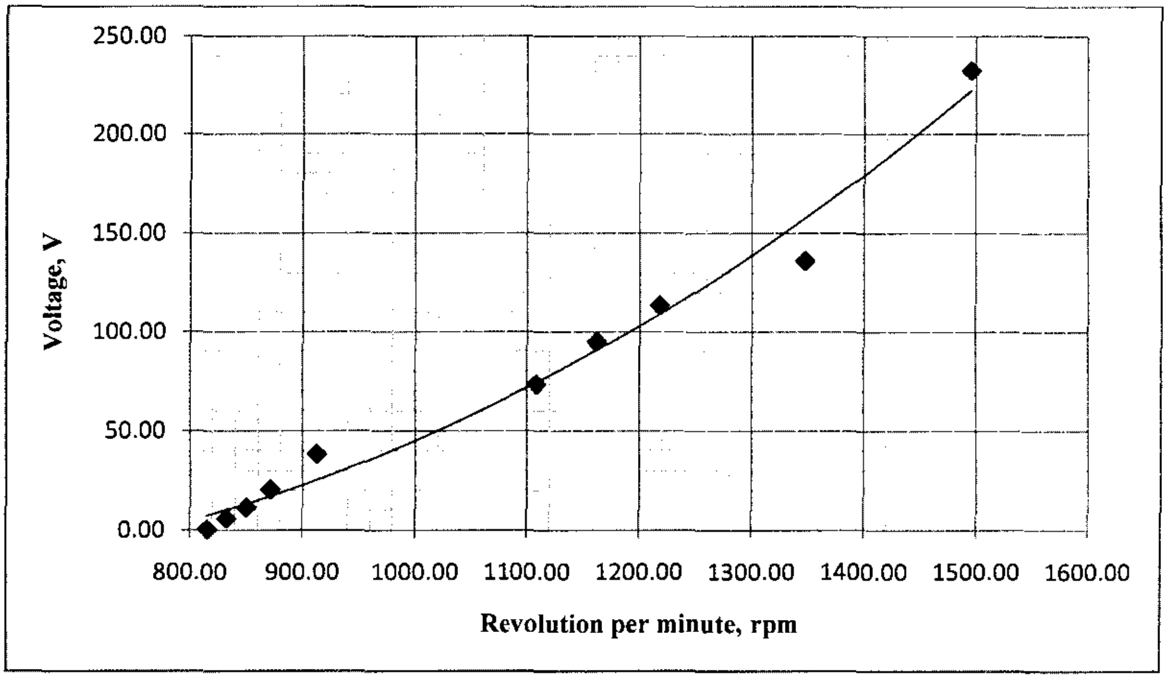

Figure 4.7: Graph of voltage (V) versus revolution per minute (rpm) for 47μF

4.3.3 Case 3: 68μF

In this case, the experiment was conducted for 68μF. The result that obtained from this experiment is shown in table 4.7.

Table 4.7: Voltage that generated by FESS for a short period (68μF)

Time, ds	Voltage, V			
	1st reading	2nd reading	3rd reading	Average
0	171.3	179.2	175.3	175.27
5	126.3	132.6	129.3	129.40
10	114.6	108.4	110	111.00
15	91.3	95.3	90.3	92.3
20	58.3	55.3	54.3	55.97
25	33.2	31.2	30.2	31.53
30	21.3	26.8	22.3	23.47
35	11.5	7.59	10.23	9.77
40	1.3	1.23	0.59	1.04

Figure 4.8 shows that, the graph of voltage (V) against time (ds). The trend of this graph decreased uniformly which is same with case 1 and case 2. According to the graph, the maximum voltage that can be generated by FESS for this capacitance is about 175.27V. The voltage drop at 10 ds and 15 ds are 111V and 92.3V respectively. For this case, the voltage generated up to 40 ds which is 1.04V. When compared to the 33μF and 47μF, the maximum voltage that generated for this case is low. This is because the 68μF absorb some energy by itself. So, the generated voltage is low compared to other two cases.

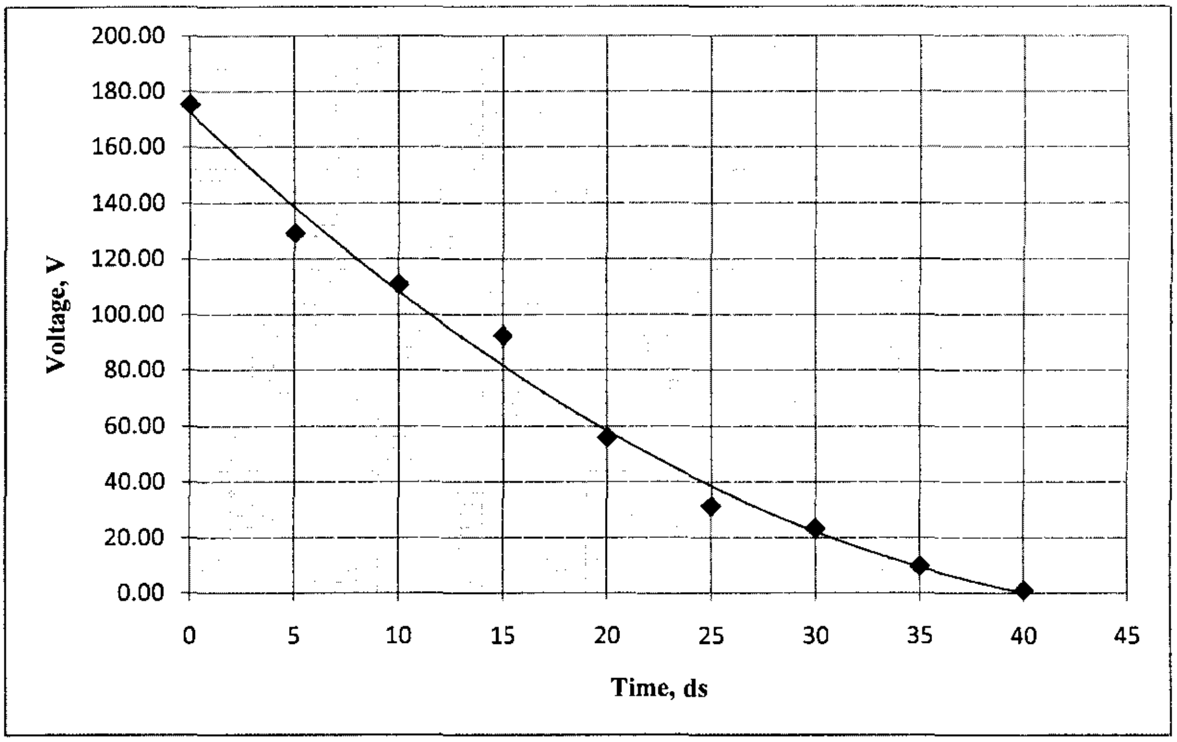

Figure 4.8: Graph of voltage (V) against time (ds) for 68μF

Table 4.8 shows, decreasing of generated voltage with speed of flywheel rotor. The result that obtained from this experiment was plotted as shown in figure 4.9. Based on this graph, the voltage decreases uniformly with decreases of the speed of flywheel rotor. At the speed of 1495 rpm the FES able to generated voltage about 173.8V and it was decreased to 60.23 at 1207.67 rpm. When the flywheel rotor rotated at the speed of 860.33 rpm, the voltage decreased to 1.1V. At the end of this experiment, the generated voltage drop to 0V.

Table 4.8: Drop of generated voltage with speed of flywheel rotor (68μF)

Voltage, V				Revolution per minute, rpm			
1st reading	2nd reading	3rd reading	Average	1st reading	2nd reading	3rd reading	Average
171.3	179.2	170.9	173.80	1497	1493	1495	1495.00
132.6	128.3	126.3	129.07	1468	1462	1461	1463.67
98.6	92.4	96.5	95.83	1352	1368	1372	1364.00
60.3	59.1	61.3	60.23	1206	1207	1210	1207.67
30.4	35.2	32.7	32.77	1106	1098	1087	1097.00
15.6	17.3	19.6	17.50	938	941	945	941.33
6.2	6.7	8.2	7.03	902	895	891	896
0.6	1.2	1.5	1.1	869	851	861	860.33

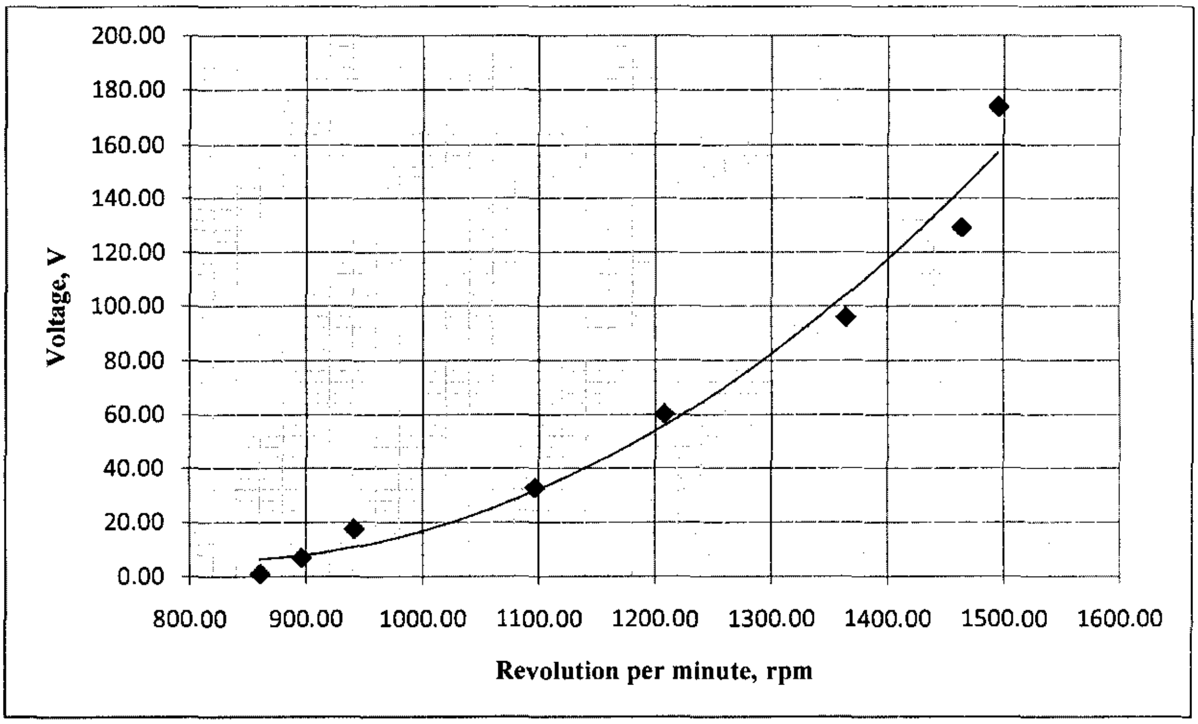

Figure 4.9: Graph of voltage (V) versus revolution per minute (rpm) for 68μF

4.4 COMPARISON BETWEEN MOTOR AND GENERATOR MODES

Based on the experiment, the duration of free rotation of flywheel rotor in motor mode is higher than generator mode. This is because, in motor mode an electrical energy applied to the stator winding is converted to torque and applied to the rotor, causing the flywheel rotor to spin faster and gain kinetic energy. While in generator mode, kinetic energy that stored in spinning flywheel applies a breakdown torque oppose the direction of the rotor. So when blackout occurs, the duration of free rotation of flywheel rotor is lower in generator mode. Breakdown torque is not the same in motor and generator modes. Generally, breakdown torque in generator mode is two to four times greater than the motor breakdown torque. For the same torque value the generated rotor losses in the generator mode operation significantly lower than in the motor mode of operation. Consequently, the nominal power of the same induction machine in the generator mode operation can be significantly higher than in the motor mode of operation.

Furthermore, existence of mechanical loses such as friction and windage losses also causing the free rotation of flywheel rotor are lower in generator mode. The FESS able to generate voltage in generator mode because the kinetic energy that stored in flywheel rotor applies a torque and it converted to an electrical energy. So, the system able to generate voltage and supplied to the critical load. Besides that, when the moment of inertia of flywheel rotor is high, the energy that stored will increase. So, it generates more electrical energy to the system.

4.5 CONCLUSION

Based on comparison done on the capacitance that used in this study, capacitance of 47μF definitely came up as the most suitable capacitance for SEIG, followed by 33μF and 68μF. The voltage generated by FESS is fully depends on properties of flywheel rotor and induction machine that used.

This chapter presented, discussed and compared data on voltage generated in different value of capacitance for SEIG. With the results gained, all the objectives of this study have been achieved accordingly. The next chapter discusses on recommendations of curative actions that could be applied in order to improve the efficiency of the system. Upon completing the next chapter, this study could be concluded as a whole.

CHAPTER 5

CONCLUSION AND RECOMMENDATIONS

5.1 CONCLUSION

The previous chapter (chapter 4) clearly discussed the results obtained from this study. Throughout this study has successfully achieved all the objectives.

First objective has been successfully achieved where a simple FESS was implemented. The induction machine was applied a concept of SEIG. Moreover, the system successfully was acting as motor and generator. The experiment shows the FESS can deliver an emergency power to a critical load. It can be said that, the induction machine has been selected due to its advantages compared to other machines.

Secondly, the period of voltage generated by FESS to critical load successfully analyzed. FESS shows potential to store energy for short period. Here, the period of voltage generated fully depends on properties of flywheel rotor and induction machine. When the moment of inertia of flywheel rotor is high the duration of flywheel to rotate is also high. Furthermore, the fast rotation of flywheel rotor is suitable for direct generation of high voltage. So, the FESS induced power to the critical load for longer time.

Finally, there are three different value of capacitors are practiced in this paper to find a minimum capacitance for SEIG. Based on experiment done, it can be concluded the capacitance of 47μF is a suitable candidate for this system and it followed by 33μF and 68μF. It can be said, FESS using SEIG has been studied. Last but not least, this system is simple and cheaper to other energy storage systems.

5.2 RECOMMENDATIONS

With respect to the limitation of this study, several recommendations could be made for the future studies pertaining flywheel energy storage system.

Frictionless or low mechanical losses of FESS would be a better representation of an efficient energy storage system. Future researches should conduct by using a vacuum chamber. The flywheel rotor should be placed into the vacuum chamber to reduce the mechanical losses and also to produce more output. Besides that, to improve the efficiency of the FESS the flywheel rotor can be fabricated in disc shape which has a shape factor of 1. So, the flywheel will rotate more rotation with faster.

As for analysis methods, an advance tachometer is highly recommended for faster results. Nevertheless, regardless of the analysis method used, a proper laboratory technique and handling would ensure results with high precision regardless of the methods used.

APPENDIX A

ANALYSIS OF MECHANICAL DESIGN

Appendix A.1 Calculation for moment of inertia and energy stored in flywheel rotor

Table A.1 Properties of flywheel rotor

Properties of flywheel rotor	
Shape	Thin firm
Material	Aluminum 1000 series
Density of Aluminum	2700 kg/m^3
Shape factor	0.5
Mass	5.2 kg
Moment of inertia	0.075 kg/m^2

The amount of energy stored in a flywheel can be calculated by using equation (2.1),

$$E_k = \frac{1}{2} I\omega^2$$

Where moment of inertia for solid cylinder is,

$$I = \frac{1}{2} mr^2 \qquad (3.3)$$

Where the mass of flywheel rotor is 5.2 kg and the radius of the flywheel is 170 mm. So, the moment of inertia of the flywheel is,

$$I = \frac{1}{2}(5.2\text{ kg})(0.17\text{m})^2$$

$$= 0.075\text{ kg.m}^2$$

So, the expected kinetic energy that will stored in the flywheel is,

$$E_k = \frac{1}{2}(0.075\ \mathrm{kg.m^2})\ (151.8\ \mathrm{rad/s})^2$$

$$= 865.73\ \mathrm{kJ}$$

The lighter material which develops lower inertial loads at a given speed with low density and high tensile strength is good for storing kinetic energy. According to equation (2.2) the maximum energy density respect to volume and mass respectively is:

$$e_v = K\sigma$$

$$= (0.5)\ (250\ \mathrm{MPa})$$

$$= 125\ \mathrm{MPa}$$

$$e_m = \frac{K\sigma}{\rho}$$

$$= \frac{(0.5)(250\ \mathrm{MPa})}{2700\ \mathrm{kg.m^3}}$$

$$= 0.0463\ \mathrm{MPa/kg.\ m^3}$$

*Where the density and tensile strength are taken from the book of Shigley's Mechanical Design Ninth Edition.

Appendix A.2 Calculation for rotor speed and torque of induction machine

Table A.1: Parameters of induction machine

Parameters of induction machine, MarelliMotori ITALY	
Model	80MB4
Power	0.75 kW
Voltage, Y	415 V
Voltage, Δ	240 V
Current, Y	1.86 A
Current, Δ	3.21 A
Phase	3
Power Factor, cos Φ	0.94
Frequency	50 Hz
R.P.M	1450
Pole	4
Mass	9.1 kg

Source: Laboratory of Electrical Drive System

According to the equation (1.4), the synchronous speed of motor is,

$$n_{sync} = \frac{120 f_e}{P} \tag{3.1}$$

$$= \frac{120(50 \text{ Hz})}{4}$$

$$= 1500 \text{ r/min}$$

$$\omega_{sync} = (1500 \text{ r/min})\ (2\pi \text{ rad/1 rev})\ (1 \text{ min/60s})$$

$$= 157.1 \text{ rad/s}$$

From the table 3.1, the rotor speed is 1450 r/min,

$$\omega_m = (1450 \text{ r/min}) (2\pi \text{ rad/1 rev}) (1 \text{ min/60s})$$

$$= 151.8 \text{ rad/s}$$

According to the equation (1.6), the shaft load torque is,

$$\tau_{ind} = \frac{P_{out}}{\omega_m} \tag{3.2}$$

$$= \frac{(15 \text{x} 1000 \text{ W})}{151.8 \text{ rad /sec}}$$

$$= 98.81 \text{ N-m}$$

Appendix A.3 Technical data of induction machine

MarelliMotori S.p.A.

PART OF THE FKI GROUP OF COMPANIES

Via Sabbionara, 1
36071 Arzignano
Vicenza
Italy

DATI TECNICI - TECHNICAL SPECIFICATION

Cliente Customer		ns. Riferimento Our Reference no.	

MOTORE TIPO - MOTOR TYPE		MA80MB4
POTENZA NOMINALE - RATED POWER	KW	0,75
SERVIZIO - DUTY TYPE		S1
TENSIONE STATORE - RATED VOLTAGE	V	400 STAR
FREQUENZA - FREQUENCY	Hz	50
CORRENTE NOMINALE STATORE - NOMINAL CURRENT	A	2
VELOCITA' NOMINALE - RATED SPEED	R.P.M.	1385
ESECUZIONE-EXECUTION		T.E.F.C.
FORMA - SHAPE	IM	IM B3 (IM 1001)
GRADO di PROTEZIONE - PROTECTION DEGREE	IP	55
TIPO di RAFFREDDAMENTO - COOLING SYSTEM	IC	411
INERZIA - INERTIA $(J = PD^2 / 4)$	Kgm^2	0,0016
TEMPERATURA AMBIENTE - AMBIENT TEMPERATURE	°C	40
CLASSE di ISOLAMENTO - INSULATION CLASS		F
CLASSE di SOVRATEMPERATURA - TEMP.RISE CLASS		B
NORME APPLICABILI - APPLICABLE STANDARDS		CEI EN 60034-1

			CARICO - LOAD
			4/4
RENDIMENTO - EFFICIENCY		%	73,2
COS Φ – POWER FACTOR			0,73
CORRENTE di C.C. - LOCKED ROTOR CURRENT		p.u.	4,1
COPPIA MASSIMA-BREAK DOWN TORQUE		p.u.	2,8
COPPIA DI SPUNTO - STARTING TORQUE		p.u.	2,8
PROTEZIONI TERMICHE THERMAL	AVVOLGIMENTI - WINDINGS		-
	CUSCINETTI - BEARINGS		-
SCALDIGLIE ANTICONDENSA - SPACE HEATERS			-

TIPO CUSCINETTI - BEARINGS	L.A. - D-END		6204-2Z
	L.O. - N-END		6204-2Z
LUBRIFICANTE -	TIPO - TYPE		-
	INTERVALLO - INTERVAL	hr	-
SENSO di ROTAZIONE - DIRECTION of ROTATION			BOTH
RUMOROSITA' - NOISE (no load operat. at 1m with tolerance 3 dB(A))		dB(A)	49
PESO - WEIGHT		Kg	9,5
INTENSITA' di VIBRAZIONE-VIBRATION LEVEL		IEC 34-14	STANDARD
COLORE FINALE - PAINTING		RAL	5010

APPENDIX B

CHARACTERISTICS OF INDUCTION MACHINE (MATLAB)

Appendix B.1 Simulink of the induction motor

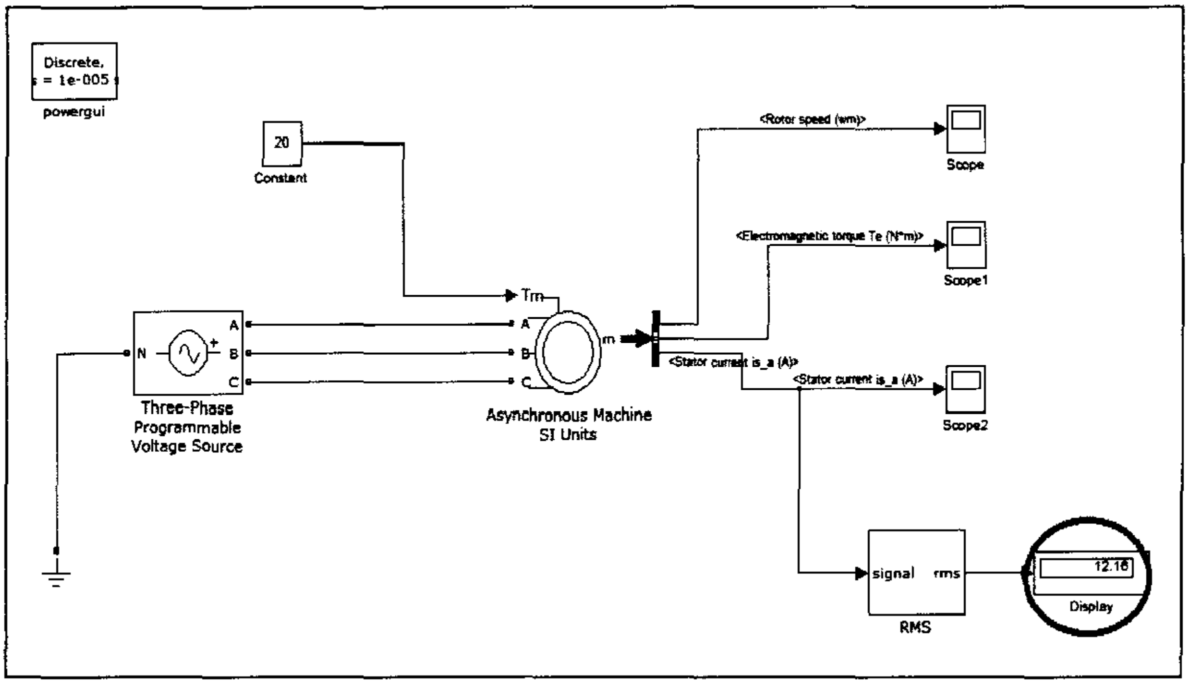

Appendix B.2 Starting condition of induction machine

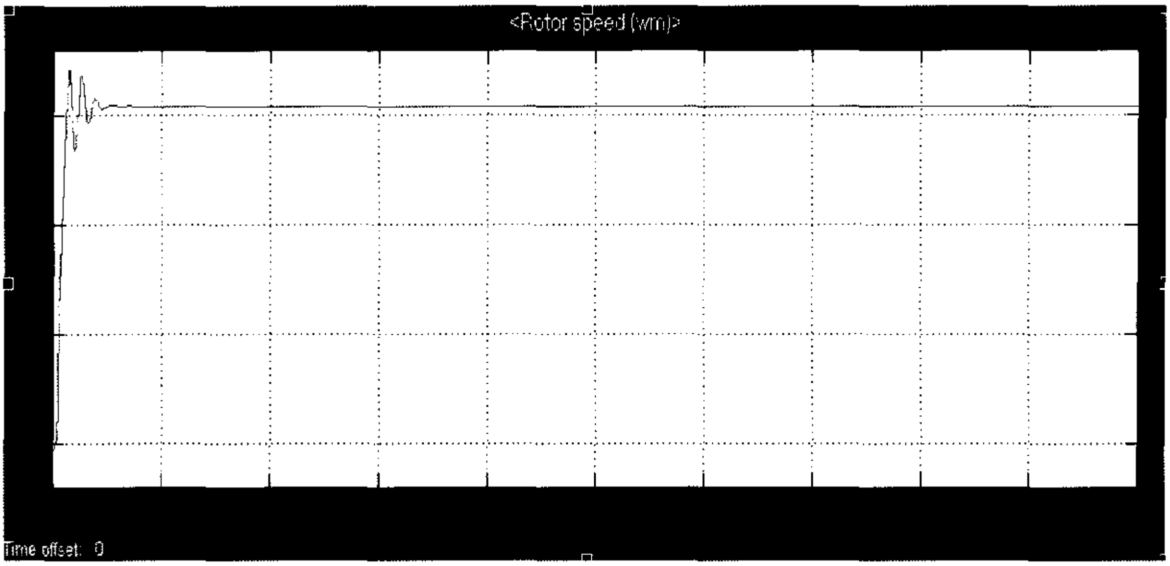

Rotor Speed

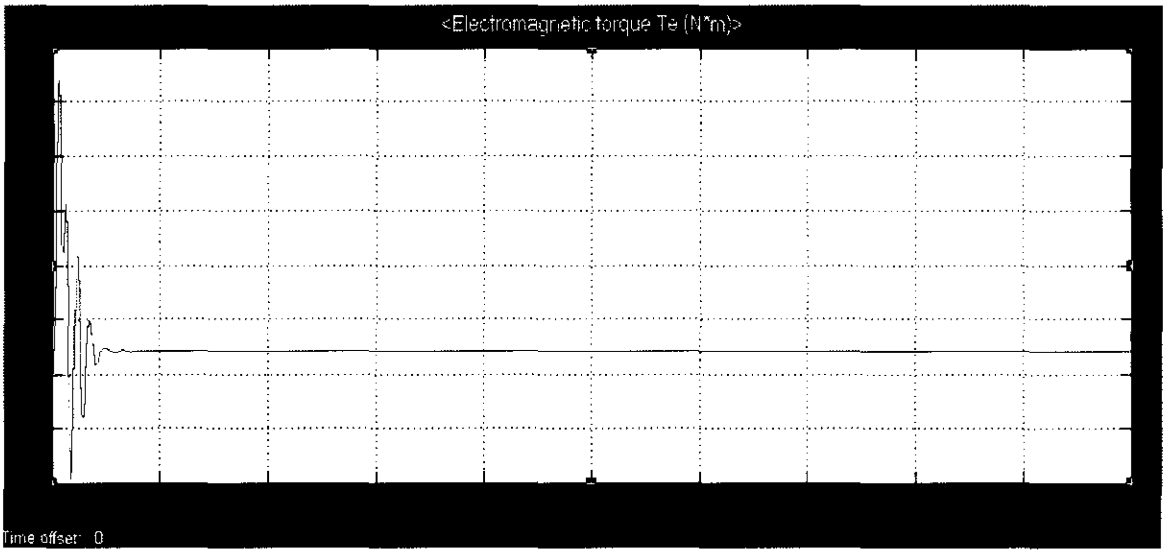

Electromagnetic Torque

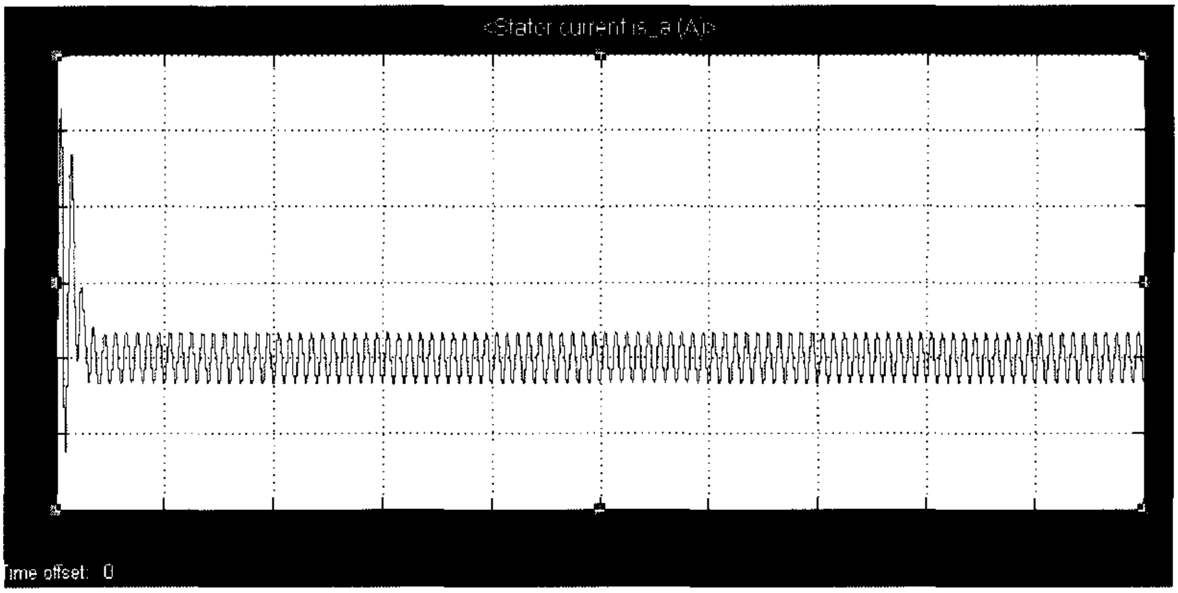

Stator Current

APPENDIX C

TECHNICAL DRAWING

Appendix C.1 Technical drawing of flywheel rotor

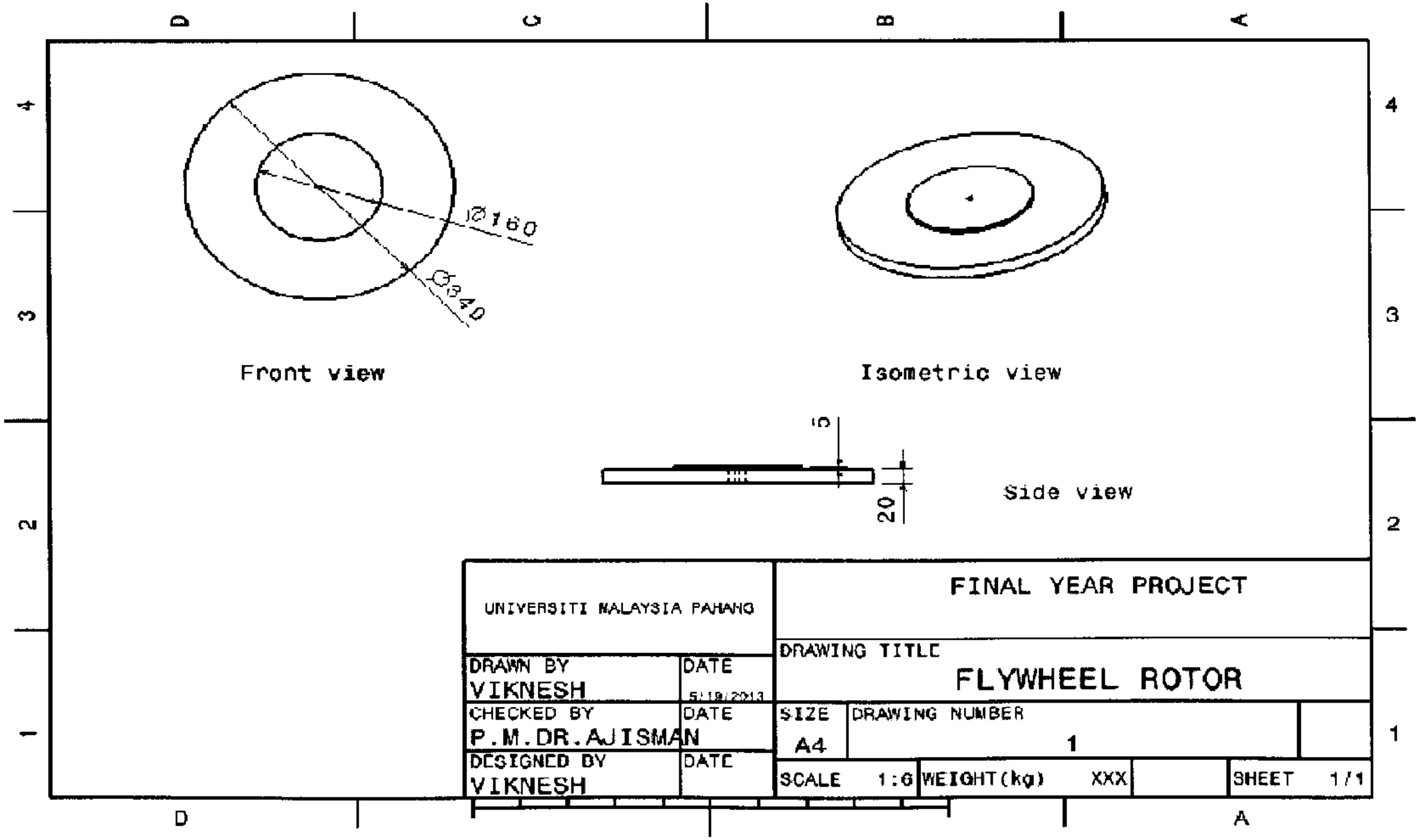

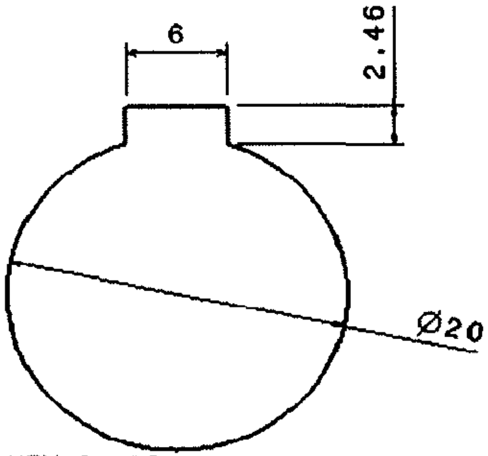

KEY SHAPE

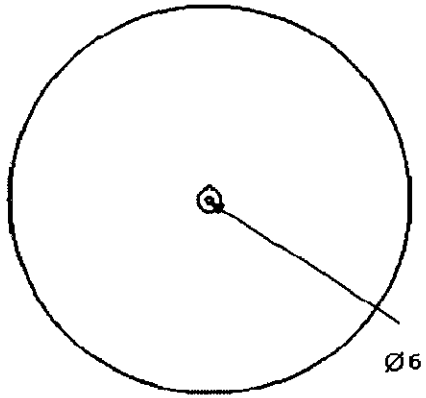

Back view

UNIVERSITI MALAYSIA PAHANG		FINAL YEAR PROJECT			
DRAWN BY VIKNESH	DATE 11/4/2013	DRAWING TITLE FLYWHEEL ROTOR			
CHECKED BY PM.DR.AJISMAN	DATE	SIZE A4	DRAWING NUMBER Part 2		REV X
DESIGNED BY VIKNESH	DATE xxx	SCALE 1:1			SHEET 1/1

Appendix C.2 Technical drawing of experiment bench

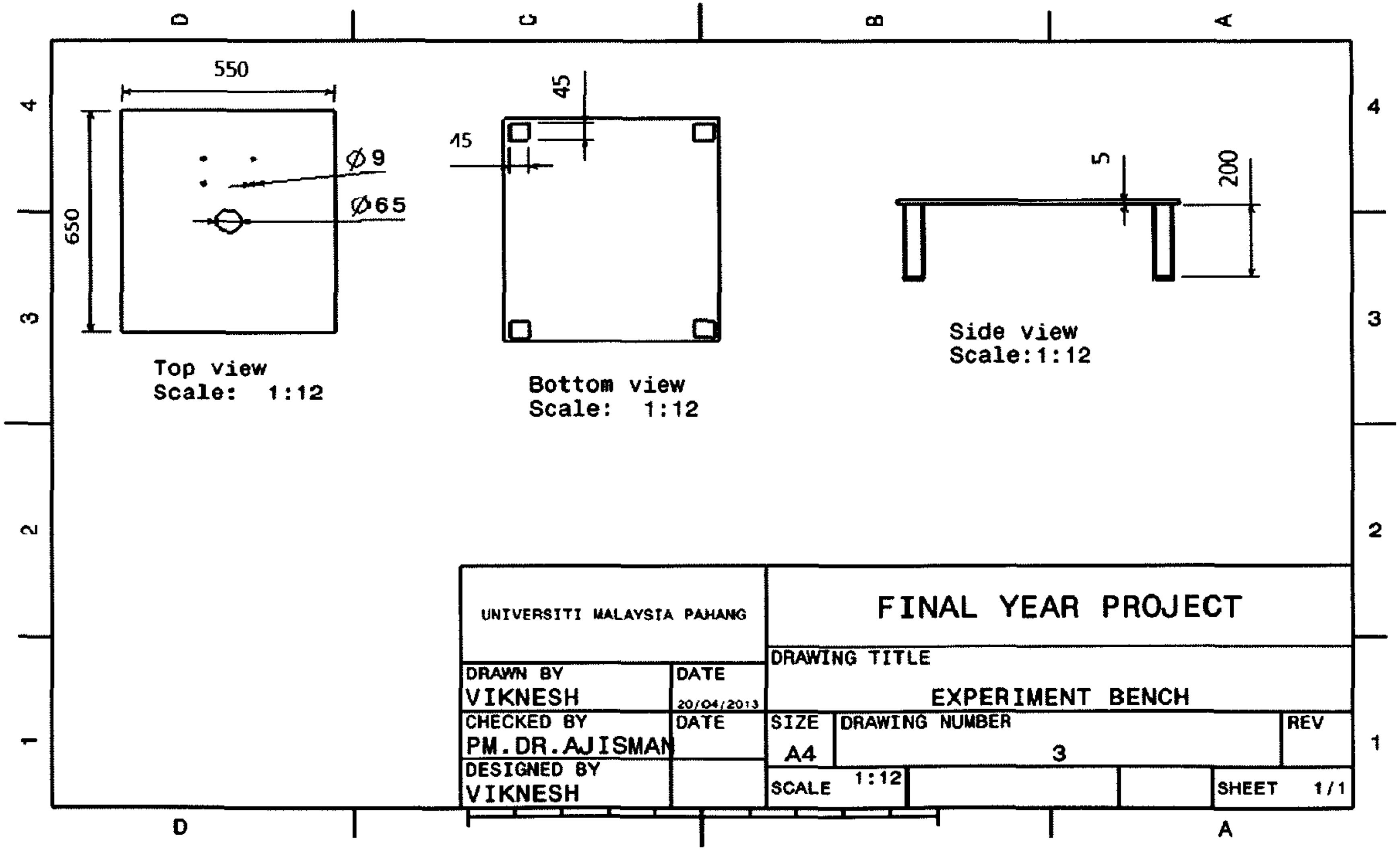

Appendix C.3 Isometric views of mechanical part

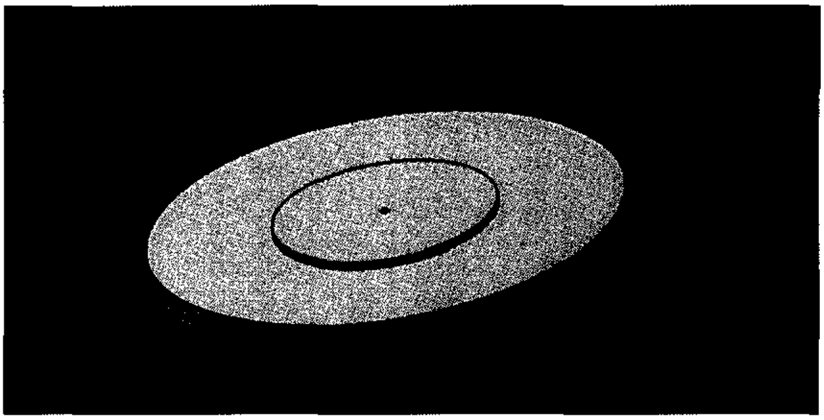

Top of flywheel rotor

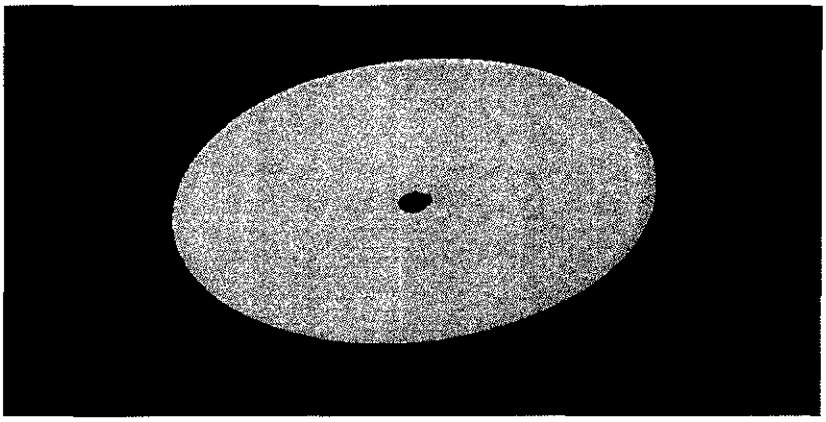

Bottom of flywheel rotor

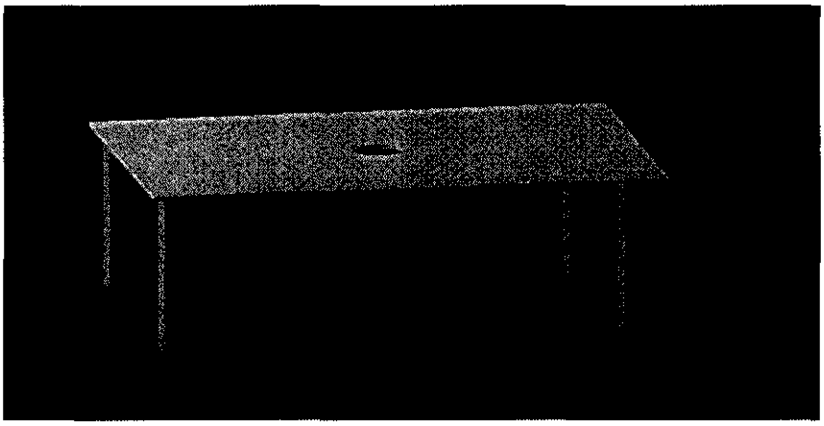

Experiment bench

3 phase induction machine

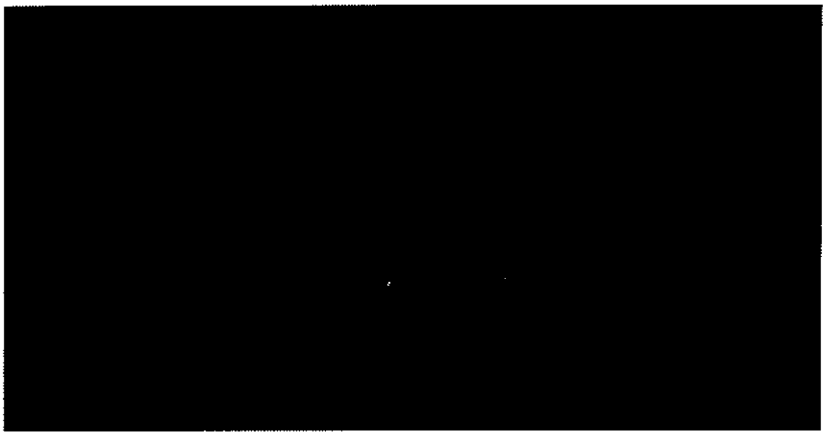

FESS

APPENDIX D

G – CODE GENERATED BY CATIA

Appendix D.1 G-code of the pocketing process

```
%(POCKET)
O1000
N1 G17 G40 G49 G54 X0 Y0 Z50.G80 G90
N2 G21
( End Mill D10 Rc0 Long )
N3 T1 S1000 M3
N10 G70 G90
:12 T2 M6
N14 G40 G90 G94
N16 G91 G74 X0 Z0
:18 G40 G90 G94
N20 G94 G97 G54 G40 G1 X-30 Z-172.3021 F39.3701 S70 H01 M3 M8
N22 Z-172.6357
N24 Z-173.4326
N26 Z-174.7118
N28 Z-176.0797
N30 Z-177.1153
N32 Z-177.5
N34 Z-177.1153
N36 Z-176.0797
N38 Z-174.7118
N40 Z-173.4326
N42 Z-172.6357
N44 Z-172.3021
N46 Z-171.1756
N48 Z-170.049
N50 Z-170.2714
N52 Z-171.1944
N54 Z-172.6456
N56 Z-174.4235
N58 Z-176.2815
N60 Z-177.9616
N62 Z-179.2307
N64 Z-179.9125
N66 Z-179.2307
N68 Z-177.9616
N70 Z-176.2815
N72 Z-174.4235
N74 Z-172.6456
```

```
N76 Z-171.1944
N78 Z-170.2714y
N80 Z-169.3425
N82 Z-170.049
N84 Z-168.9225
N86 Z-167.7959
N88 Z-167.9071
N90 Z-168.9991
N92 Z-170.6715
N94 Z-172.7627
N96 Z-175.0702
N98 Z-177.371
N100 Z-179.4424
N102 Z-181.0841
N104 Z-182.1372
N106 Z-182.5
N140 M5
N142 M30
N144 M2
N146 G91 G74 X0 Z0
N148 M2
%
```

Appendix D.2 G-code of drilling process

```
%(DRILLING)
O2000
N1 G17 G40 G49 G54 X0 Y0 Z50.G80 G90
N2 G21
( End Mill D6 Rc0 Long )
N3 T1 S1000 M3
N14 G40 G90 G94
N16 G91 G74 X0 Z0
:18 G40 G90 G94
N20 G97 G54 G40 G0 X-1 Z0 S70 H01 M3
N22 G94 G1 X10 F39.3701 M8
N24 X-1
N26 X15
N28 X-1
N30 M5
N32 M30
N34 M2
N36 G91 G74 X0 Z0
N38 M2
%
```

Appendix D.3 G-code of roughing process

```
%(ROUGHING)
O4000
N1 G17 G40 G49 G54
X0 Y0 Z50.G80 G90
N2 G21
( End Mill D20 Rc0
Long )
N3 T1 S1000 M3
N10 G70 G90
N14 G40 G90 G94
N16 G91 G74 X0 Z0
:18 G40 G90 G94
N20 G97 G54 G40 G0
X65 Z9.0153 S70
H01 M3
N22 X.1
N24 G94 G1 X-17.5
F11.811 M8
N26 Z0
N28 Z-137.8557
F39.3701
N30 Z-132.7803
N32 Z-132.6602
N34 Z-127.6331
N36 Z-127.5218
N38 Z-121.328
N40 Z-121.2496
N42 Z-114.3226
N44 Z-114.1682
N46 Z-106.2232
N48 Z-106.083
N50 Z-96.4503
N52 Z-96.2961
N54 Z-90.1952
N56 Z-90.1075
N58 Z-83.8164
N60 Z-83.7176
N62 Z-77.7914
N64 Z-77.6727
N66 Z-69.2493
N68 Z-69.103
N70 Z-62.971
N72 Z-62.9522
N74 Z-61.0328
N76 Z-60.9185
N78 Z-53.8153
N80 Z-53.685
N82 Z-46.1985
N84 Z-46.0948
N86 Z-41.9777
N88 Z-41.9151
N90 Z-37.1628
N92 Z-37.0961
N94 Z-32.6598
N96 Z-32.5737
N98 Z-28.4699
N100 Z-28.4188
N102 Z-26.6136
N104 Z-26.555
N106 Z-22.7833
N108 Z-22.7748
N110 Z-21.1584
N112 Z-21.0786
N114 Z-16.3931
N116 Z-16.3176
N118 Z-11.9147
N120 Z-11.8469
N122 Z-9.4478
N124 Z-9.4181
N126 Z-6.8063
N128 Z-6.7695
N130 Z-4.3807
N132 Z-4.3378
N134 Z-2.4397
N136 Z-2.4164
N138 Z-1.5455
N140 Z-1.5193
N142 Z-.0524
N144 Z-.0495
N146 Z0
N148 Z-2.5
N150 Z-5
N152 Z-104.6465
N154 Z-104.6389
N156 Z-112.721
N158 Z-104.6575
N160 Z-104.65
N162 Z-104.4032
N164 Z-104.1687
N166 Z-94.3958
N168 Z-94.1401
N170 Z-87.8849
N172 Z-87.7368
N174 Z-81.3581
N176 Z-81.1938
N178 Z-75.1688
N180 Z-74.971
N182 Z-66.4289
N184 Z-66.3043
N186 Z-66.158
N188 Z-66.0374
N190 Z-59.9054
N192 Z-59.8743
N194 Z-57.9361
N196 Z-57.7469
N198 Z-50.5294
N200 Z-50.4179
N202 Z-50.2876
N204 Z-50.1806
N206 Z-42.694
N208 Z-42.5232
N210 Z-38.3024
N212 Z-38.1967
N214 Z-33.3819
N216 Z-33.2707
N218 Z-28.7677
N220 Z-28.6249
N222 Z-24.435
N224 Z-24.3496
N226 Z-22.4933
N228 Z-22.3952
N230 Z-18.5648
N232 Z-18.55
N234 Z-16.9252
N236 Z-16.7931
N238 Z-12.0279
N240 Z-11.898
N242 Z-7.4196
N244 Z-7.3041
N246 Z-5.0198
N248 Z-5.0585
N250 Z-3.4808
N252 Z-4.9602
N254 Z-5
N256 Z-7.5
N258 Z-10
N260 Z-82.9771
N262 Z-82.9678
N264 Z-88.0683
N266 Z-82.9932
```

```
N268 Z-82.9838

N270 Z-78.9014
N272 Z-78.7376
N274 Z-72.5483
N276 Z-72.4465
N278 Z-72.2487
N280 Z-72.1506
N282 Z-63.6085
N284 Z-63.5122
N286 Z-63.2413
N288 Z-63.0936
N290 Z-56.841
N292 Z-56.809
N294 Z-54.8397
N296 Z-54.7439
N298 Z-54.5546
N300 Z-54.461
N302 Z-47.2435
N304 Z-47.1573
N306 Z-46.9155
N308 Z-46.7839
N310 Z-39.1903
N312 Z-39.103
N314 Z-38.9322
N316 Z-38.848
N318 Z-34.6272
N320 Z-34.5226
N322 Z-29.602
N324 Z-29.4911
N326 Z-24.8769
N328 Z-24.8031
N330 Z-24.6603
N332 Z-24.59
N334 Z-20.4001
N336 Z-20.3165
N338 Z-18.3747
N340 Z-18.276
N342 Z-14.3475
N344 Z-14.3316
N346 Z-12.692
N348 Z-12.6244
N350 Z-12.4925
N352 Z-12.4279
N354 Z-10.0252
N356 Z-10.061
N358 Z-8.6723
N360 Z-9.9642
N362 Z-10
N364 Z-12.5
N366 Z-15
N368 Z-65.4193
N370 Z-65.4091
N372 Z-69.201
N374 Z-65.4386
N376 Z-65.4284
N378 Z-60.7887
N380 Z-60.7043
N382 Z-60.337
N384 Z-60.1785
N386 Z-53.7783
N388 Z-53.7448
N390 Z-51.7435
N392 Z-51.6633
N394 Z-51.3783
N396 Z-51.2693
N398 Z-43.9582
N400 Z-43.8825
N402 Z-43.5545
N404 Z-43.4128
N406 Z-35.6876
N408 Z-35.6138
N410 Z-35.3558
N412 Z-35.2578
N414 Z-30.9527
N416 Z-30.8484
N418 Z-25.8232
N420 Z-25.7125
N422 Z-20.9874
N424 Z-20.9246
N426 Z-20.708
N428 Z-20.6259
N430 Z-16.3657
N432 Z-16.2832
N434 Z-15.0298
N436 Z-15.0624
N438 Z-13.8198
N440 Z-14.9667
N442 Z-15
N444 Z-17.5
N446 Z-20
N448 Z-50.2118
N450 Z-50.2012
N452 Z-53.2642
N454 Z-50.2336
N456 Z-50.2231
N458 Z-48.6477
N460 Z-48.5759
N462 Z-48.2106
N464 Z-48.0937
N466 Z-40.6737
N468 Z-40.6042
N470 Z-40.2005
N472 Z-40.0531
N474 Z-32.1862
N476 Z-32.1192
N478 Z-31.7874
N480 Z-31.6824
N482 Z-27.2793
N484 Z-27.1749
N486 Z-22.0455
N488 Z-21.9349
N490 Z-20.0333
N492 Z-20.0638
N494 Z-18.9831
N496 Z-19.9696
N498 Z-20
N500 Z-22.5
N502 Z-25
N504 Z-36.7003
N506 Z-36.6893
N508 Z-39.2601
N510 Z-36.7247
N512 Z-36.7146
N514 Z-36.7004
N516 Z-28.6861
N518 Z-28.6233
N520 Z-28.2245
N522 Z-28.1152
N524 Z-25.0365
N526 Z-25.0648
N528 Z-24.0463
N530 Z-24.9716
N532 Z-25
N534 Z-26.2507
N536 Z-27.5013
N538 Z-27.6596
N540 Z-28
N542 Z-29.407
N544 Z-29.8699
N546 Z-29.757
N548 Z-28.35
N550 Z-27.8064
N552 Z-27.5
N554 Z-27.5013
N556 X-7.5 F.0394
N558 G0 X65
N560 Z8.1013
N562 X10.1
N564 G1 X.1
F11.811
N566 X-17.5
N568 Z-.005
```

```
N570 Z-.2441
F39.3701
N572 Z-.6494
N574 Z-2.2367
N576 Z-2.9787
N578 Z-4.4455
N580 Z-5.3164
N582 Z-7.2144
N584 Z-9.6032
N586 Z-12.215
N588 Z-14.614
N590 Z-17.22
N592 Z-19.0129
N594 Z-23.6983
N596 Z-25.3147
N598 Z-29.0865
N600 Z-30.8917
N602 Z-34.9955
N604 Z-39.4318
N606 Z-44.1841
N608 Z-48.3011
N610 Z-55.7877
N612 Z-62.8909
N614 Z-64.8103
N616 Z-70.9423
N618 Z-71.2086
N620 Z-79.3657
N622 Z-85.292
N624 Z-91.5831
N626 Z-97.684
N628 Z-107.3167
N630 Z-115.2617
N632 Z-122.1886
N634 Z-128.3823
N636 Z-133.4094
N638 Z-142.0081
N640 Z-148.4839
N642 Z-154.543
N644 Z-156.8019
N646 X-17.2194 Z-
157.7754
N648 X-16.9388 Z-
158.4421
N650 X-16.6582 Z-
158.6236
N652 X-6.6582
F.0394
N654 G0 X65
N656 Z-156.176
N658 X10.2
N660 G1 X.2
F11.811
N662 X-17.5
N664 Z-156.8601
N666 Z-165.294
F39.3701
N668 Z-174.5478
N670 Z-174.9732
N672 Z-175.2671
N674 Z-181.4249
N676 Z-188.2376
N678 Z-193.0848
N680 Z-193.3899
N682 X-7.5 F.0394
N684 G0 X65
N686 Z7.9576
N688 X10.2
N690 G1 X.2
F11.811
N692 X-17.5
N694 Z0
N696 Z.3926
F39.3701
N698 Z.888
N700 Z.9093
N702 Z.9209
N704 Z.4407
N706 Z0
N708 Z2.9828
N710 X-7.5 F.0394
N712 G0 X65
N714 Z9.0153
N716 X-7.4
N718 G1 X-17.4
F11.811
N720 X-35
N722 Z0
N724 Z-137.4985
F39.3701
N726 Z-134.8719
N728 Z-134.7461
N730 Z-132.6851
N732 Z-132.6602
N734 Z-127.6331
N736 Z-127.5218
N738 Z-121.328
N740 Z-121.2496
N742 Z-114.3226
N744 Z-114.1682
N746 Z-106.2232
N748 Z-106.1645
N750 Z-104.3728
N752 Z-104.2709
N754 Z-96.4503
N756 Z-96.2959
N758 Z-95.8274
N760 Z-95.7339
N762 Z-95.2205
N764 Z-95.1619
N766 Z-91.8074
N768 Z-91.6772
N770 Z-87.0326
N772 Z-86.9556
N774 Z-86.1847
N776 Z-86.1455
N778 Z-81.4821
N780 Z-81.3575
N782 Z-78.2988
N784 Z-78.2491
N786 Z-77.6243
N788 Z-77.5294
N790 Z-71.7911
N792 Z-71.6693
N794 Z-69.2204
N796 Z-69.103
N798 Z-61.8645
N800 Z-61.7741
N802 Z-60.9807
N804 Z-60.9185
N806 Z-53.8153
N808 Z-53.7276
N810 Z-52.6339
N812 Z-52.5494
N814 Z-52.0724
N816 Z-52.0173
N818 Z-46.1985
N820 Z-46.0948
N822 Z-44.9304
N824 Z-44.8985
N826 Z-43.6859
N828 Z-43.5026
N830 Z-39.1841
N832 Z-39.008
N834 Z-32.9745
N836 Z-32.9196
N838 Z-32.6101
N840 Z-32.5737
N842 Z-28.4699
N844 Z-28.4188
N846 Z-26.6136
N848 Z-26.555
N850 Z-21.7894
```

```
N852 Z-21.7309
N854 Z-21.1231
N856 Z-21.0786
N858 Z-16.3931
N860 Z-16.3437
N862 Z-15.521
N864 Z-15.4748
N866 Z-11.9147
N868 Z-11.8776
N870 Z-11.6608
N872 Z-11.6282
N874 Z-10.3558
N876 Z-10.2908
N878 Z-6.1189
N880 Z-6.0799
N882 Z-5.9191
N884 Z-5.8902
N886 Z-4.3782
N888 Z-4.3378
N890 Z-2.4397
N892 Z-2.4164
N894 Z-1.5455
N896 Z-1.5191
N898 Z0
N900 Z-2.5
N902 Z-5
N904 Z-104.6465
N906 Z-104.6389
N908 Z-112.721
N910 Z-104.6575
N912 Z-104.65
N914 Z-104.4032
N916 Z-104.3045
N918 Z-102.4541
N920 Z-102.2873
N922 Z-94.3648
N924 Z-94.3157
N926 Z-93.6928
N928 Z-93.5511
N930 Z-89.5311
N932 Z-89.4222
N934 Z-84.6474
N936 Z-84.5615
N938 Z-83.7137
N940 Z-83.6429
N942 Z-78.9403
N944 Z-78.815
N946 Z-74.9572
N948 Z-74.8183
N950 Z-68.9851
N952 Z-68.8811
N954 Z-66.3104
N956 Z-66.1613
N958 Z-58.8054
N960 Z-58.6884
N962 Z-57.8046
N964 Z-57.6938
N966 Z-50.5284
N968 Z-50.4184
N970 Z-49.237
N972 Z-49.1891
N974 Z-48.6276
N976 Z-48.5442
N978 Z-42.6702
N980 Z-42.5708
N982 Z-39.9091
N984 Z-39.7659
N986 Z-35.2713
N988 Z-35.1238
N990 Z-29.0903
N992 Z-29.0055
N994 Z-28.6411
N996 Z-28.5741
N998 Z-24.4339
N1000 Z-24.3496
N1002 Z-22.4933
N1004 Z-22.4001
N1006 Z-17.5758
N1008 Z-17.5014
N1010 Z-16.8352
N1012 Z-16.7572
N1014 Z-12.0272
N1016 Z-11.9468
N1018 Z-11.0746
N1020 Z-11.015
N1022 Z-7.4087
N1024 Z-7.3583
N1026 Z-7.1044
N1028 Z-7.0779
N1030 Z-5.7729
N1032 Z-5.6954
N1034 Z-5.0184
N1036 Z-5.0584
N1038 Z-3.5293
N1040 Z-4.9601
N1042 Z-5
N1044 Z-7.5
N1046 Z-10
N1048 Z-82.8176
N1050 Z-82.8085
N1052 Z-87.9927
N1054 Z-82.8331
N1056 Z-82.8239
N1058 Z-82.2633
N1060 Z-82.1802
N1062 Z-81.2465
N1064 Z-81.1723
N1066 Z-76.3989
N1068 Z-76.2751
N1070 Z-72.292
N1072 Z-72.1527
N1074 Z-66.1806
N1076 Z-66.077
N1078 Z-63.4024
N1080 Z-63.2528
N1082 Z-55.7478
N1084 Z-55.636
N1086 Z-54.6352
N1088 Z-54.5185
N1090 Z-47.2423
N1092 Z-47.1361
N1094 Z-45.8446
N1096 Z-45.794
N1098 Z-45.1846
N1100 Z-45.0999
N1102 Z-39.1426
N1104 Z-39.0617
N1106 Z-36.3005
N1108 Z-36.1744
N1110 Z-31.5367
N1112 Z-31.4598
N1114 Z-31.3123
N1116 Z-31.2395
N1118 Z-25.206
N1120 Z-25.1291
N1122 Z-24.6799
N1124 Z-24.6056
N1126 Z-20.3984
N1128 Z-20.3153
N1130 Z-18.3746
N1132 Z-18.2805
N1134 Z-13.3631
N1136 Z-13.2914
N1138 Z-12.5507
N1140 Z-12.4698
N1142 Z-10.0252
N1144 Z-10.061
N1146 G91 G74 X0
Z0
N1180M2
%
```

APPENDIX E

FLYWHEEL AND EXPERIMENT BENCH

Appendix E.1 Mechanical parts of FESS

Front view of flywheel rotor

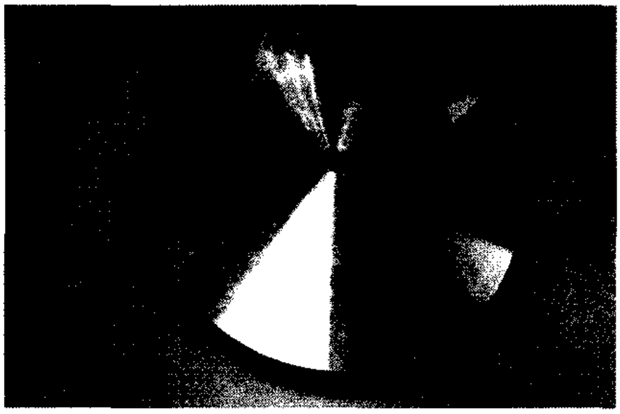

Bottom view of flywheel rotor

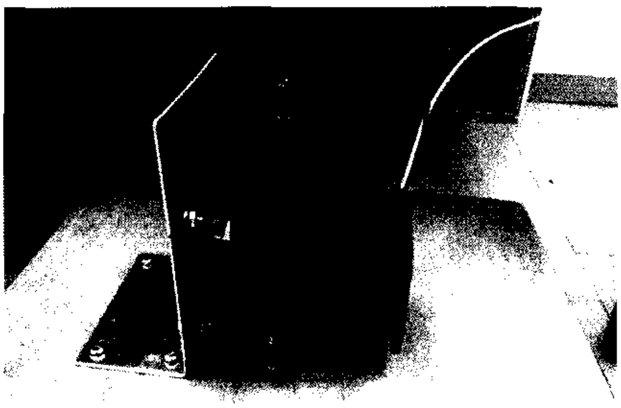

'L' shape induction machine holder

Experiment bench of FESS

APPENDIX F

DATASHEET OF ELECTRONIC COMMPONENTS

Appendix F.1 Voltage regulator, L7809

CDIL

Continental Device India Limited

An ISO/TS 16949, ISO 9001 and ISO 14001 Certified Company

3-TERMINAL POSITIVE VOLTAGE REGULATOR

LM7809

TO-220
Plastic Package

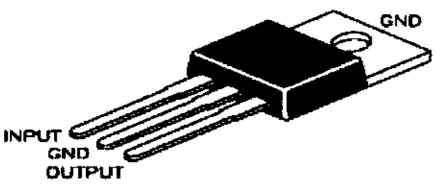

The Voltages Available allow these Regulators to be used in Logic Systems, Instrumentation, Hi-Fi Audio Circuits and other Solid State Electronic Equipment

ABSOLUTE MAXIMUM RATINGS (T_a=25°C)

DESCRIPTION	SYMBOL	VALUE	UNIT
Input Voltage	V_{IN}	35	V
		40	
Power Dissipation	P_D	15	W
Operating Temperature	T_{amb}	- 20 to +80	°C
Storage Temperature Range	T_{stg}	- 55 to +150	°C

ELECTRICAL CHARACTERISTICS (T_a=25°C unless specified otherwise)

V_{IN}=18V, I_O=100mA, T_a=25°C

DESCRIPTION	SYMBOL	TEST CONDITION	MIN	TYP	MAX	UNIT
Output Voltage	V_O	I_O=5mA ~ 1.5A V_{IN}=12 ~ 24V, P_D 15W	8.65		9.35	V
Line Regulation	R_{EGV}	V_{IN}=11.5 ~ 26V			90	mV
Load Regulation	R_{EGL}	I_O=5mA ~ 1.5A			90	mV
Quiescent Current	I_Q				8.0	mA
Quiescent Current Change	I_Q	V_{IN}=11.5 ~ 26V			1.0	mA
		I_O=5mA ~ 1A			0.5	mA
Input Voltage	V_{IN}		11.5		26	V
Ripple Rejection Radio	R_R	V_{IN}=12 ~ 22V, f=120Hz	56			dB
Max Output Current	I_{OM}	T_J=25°C		2.2		A
Output Voltage Drift	V/T	I_O=5mA , T_J=0 ~ 125°C		- 0.5		mV/°C
Output Noise Voltage	V_{NO}	f=10Hz ~ 100KHz		10		µV
Short Circuit Current Limit	I_{SC}	T_J=25°C		2.0		A

LM7809Rev041004E

Appendix F.2 Diode, 1N4003

DIODES INCORPORATED

1N4001 - 1N4007

1.0A RECTIFIER

Please click here to visit our online spice models database.

Features

- Diffused Junction
- High Current Capability and Low Forward Voltage Drop
- Surge Overload Rating to 30A Peak
- Low Reverse Leakage Current
- **Lead Free Finish, RoHS Compliant (Note 3)**

Mechanical Data

- Case: DO-41
- Case Material: Molded Plastic. UL Flammability Classification Rating 94V-0
- Moisture Sensitivity: Level 1 per J-STD-020D
- Terminals: Finish - Bright Tin. Plated Leads Solderable per MIL-STD-202, Method 208
- Polarity: Cathode Band
- Mounting Position: Any
- Ordering Information: See Page 2
- Marking: Type Number
- Weight: 0.30 grams (approximate)

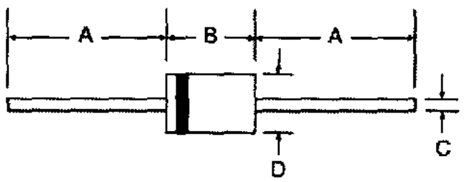

Dim	DO-41 Plastic Min	Max
A	25.40	—
B	4.06	5.21
C	0.71	0.864
D	2.00	2.72
All Dimensions in mm		

Maximum Ratings and Electrical Characteristics @T_A = 25°C unless otherwise specified

Single phase, half wave, 60Hz, resistive or inductive load.
For capacitive load, derate current by 20%.

Characteristic	Symbol	1N4001	1N4002	1N4003	1N4004	1N4005	1N4006	1N4007	Unit
Peak Repetitive Reverse Voltage Working Peak Reverse Voltage DC Blocking Voltage	V_{RRM} V_{RWM} V_R	50	100	200	400	600	800	1000	V
RMS Reverse Voltage	$V_{R(RMS)}$	35	70	140	280	420	560	700	V
Average Rectified Output Current (Note 1) @ T_A = 75°C	I_O	1.0							A
Non-Repetitive Peak Forward Surge Current 8.3ms single half sine-wave superimposed on rated load	I_{FSM}	30							A
Forward Voltage @ I_F = 1.0A	V_{FM}	1.0							V
Peak Reverse Current @T_A = 25°C at Rated DC Blocking Voltage @ T_A = 100°C	I_{RM}	5.0 50							µA
Typical Junction Capacitance (Note 2)	C_j	15				8			pF
Typical Thermal Resistance Junction to Ambient	$R_{\theta JA}$	100							K/W
Maximum DC Blocking Voltage Temperature	T_A	+150							°C
Operating and Storage Temperature Range	T_J, T_{STG}	-65 to +150							°C

Notes:
1. Leads maintained at ambient temperature at a distance of 9.5mm from the case.
2. Measured at 1.0 MHz and applied reverse voltage of 4.0V DC.
3. EU Directive 2002/95/EC (RoHS). All applicable RoHS exemptions applied, see EU Directive 2002/95/EC Annex Notes.

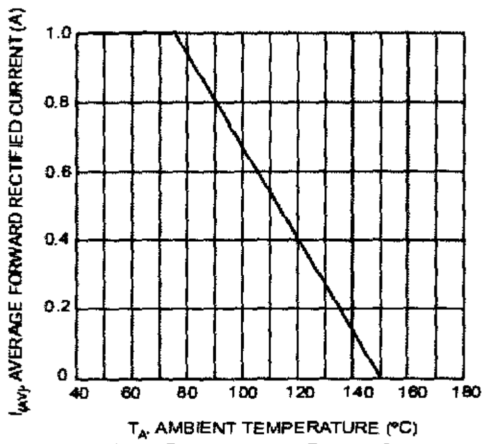

Fig. 1 Forward Current Derating Curve

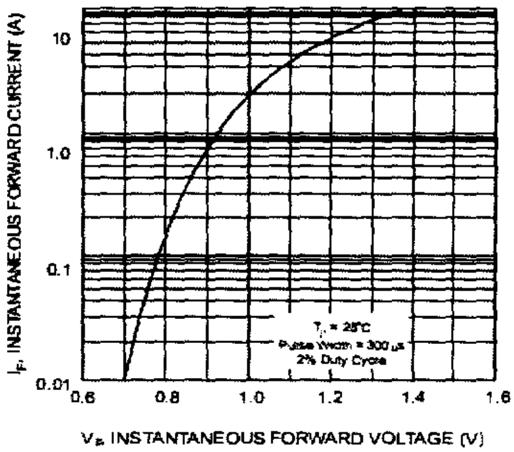

Fig. 2 Typical Forward Characteristics

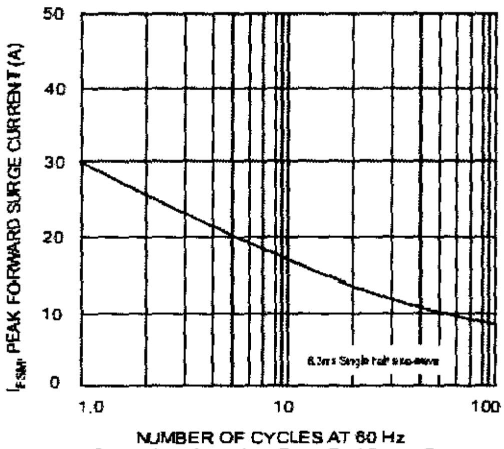

Fig. 3 Max Non-Repetitive Peak Fwd Surge Current

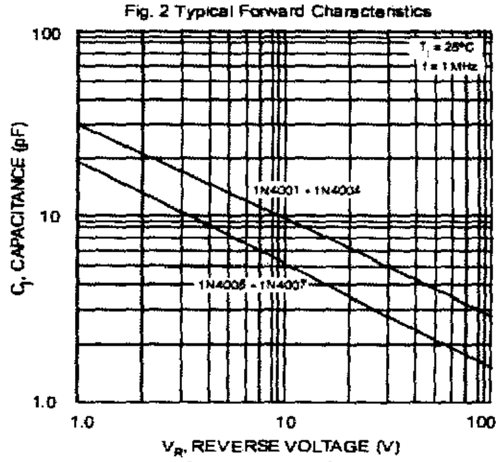

Fig. 4 Typical Junction Capacitance

Ordering Information (Note 4)

Device	Packaging	Shipping
1N4001-B	DO-41 Plastic	1K/Bulk
1N4001-T	DO-41 Plastic	5K/Tape & Reel, 13-inch
1N4002-B	DO-41 Plastic	1K/Bulk
1N4002-T	DO-41 Plastic	5K/Tape & Reel, 13-inch
1N4003-B	DO-41 Plastic	1K/Bulk
1N4003-T	DO-41 Plastic	5K/Tape & Reel, 13-inch
1N4004-B	DO-41 Plastic	1K/Bulk
1N4004-T	DO-41 Plastic	5K/Tape & Reel, 13-inch
1N4005-B	DO-41 Plastic	1K/Bulk
1N4005-T	DO-41 Plastic	5K/Tape & Reel, 13-inch
1N4006-B	DO-41 Plastic	1K/Bulk
1N4006-T	DO-41 Plastic	5K/Tape & Reel, 13-inch
1N4007-B	DO-41 Plastic	1K/Bulk
1N4007-T	DO-41 Plastic	5K/Tape & Reel, 13-inch

Notes: 4. For packaging details, visit our website at http://www.diodes.com/datasheets/ap02008.pdf

Appendix F.3 SPDT relay

SONGLE RELAY

松乐继电器 ® SONGLE RELAY	RELAY ISO9002	SRD

1. MAIN FEATURES

- Switching capacity available by 10A in spite of small size design for highdensity P.C. board mounting technique.
- UL,CUL,TUV recognized.
- Selection of plastic material for high temperature and better chemical solution performance.
- Sealed types available.
- Simple relay magnetic circuit to meet low cost of mass production.

2. APPLICATIONS

- Domestic appliance, office machine, audio, equipment, automobile, etc.
  (Remote control TV receiver, monitor display, audio equipment high rushing current use application.)

3. ORDERING INFORMATION

SRD	XX VDC	S	L	C
Model of relay	Nominal coil voltage	Structure	Coil sensitivity	Contact form
SRD	03、05、06、09、12、24、48VDC	S:Sealed type	L:0.36W	A:1 form A
				B:1 form B
		F:Flux free type	D:0.45W	C:1 form C

4. RATING

CCC	FILE NUMBER:	CQC03001003731	10A/250VDC
UL/CUL	FILE NUMBER:	E167996	10A/125VAC 28VDC
TUV	FILE NUMBER:	R50056114	10A/250VAC 30VDC

5. DIMENSION(unit:mm) DRILLING(unit:mm) WIRING DIAGRAM

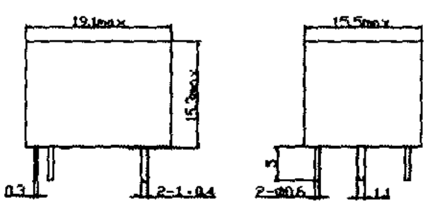

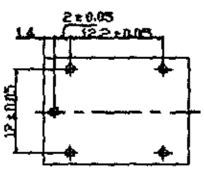

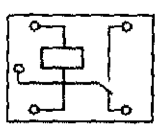

6. COIL DATA CHART (AT20°C)

Coil Sensitivity	Coil Voltage Code	Nominal Voltage (VDC)	Nominal Current (mA)	Coil Resistance (Ω) ±10%	Power Consumption (W)	Pull-In Voltage (VDC)	Drop-Out Voltage (VDC)	Max-Allowable Voltage (VDC)
SRD (High Sensitivity)	03	03	120	25	abt. 0.36W	75%Max.	10% Min.	120%
	05	05	71.4	70				
	06	06	60	100				
	09	09	40	225				
	12	12	30	400				
	24	24	15	1600				
	48	48	7.5	6400				
SRD (Standard)	03	03	150	20	abt. 0.45W	75% Max.	10% Min.	110%
	05	05	89.3	55				
	06	06	75	80				
	09	09	50	180				
	12	12	37.5	320				
	24	24	18.7	1280				
	48	48	10	4500	abt. 0.51W			

7. CONTACT RATING

Item \ Type	SRD FORM C	SRD FORM A
Contact Capacity Resistive Load (cosΦ=1)	10A 125VAC	10A 30VDC 10A 250VAC
Inductive Load (cosΦ=0.4 L/R=7msec)	3A 120VAC 3A 28VDC	5A 120VAC 5A 28VDC
Max. Allowable Voltage	250VAC/110VDC	250VAC/110VDC
Max. Allowable Power Force	800VAC/240W	1200VA/300W
Contact Material	AgCdO	AgCdO

8. PERFORMANCE (at initial value)

Item \ Type	SRD
Contact Resistance	100mΩ Max.
Operation Time	10msec Max.
Release Time	5msec Max.
Dielectric Strength Between coil & contact Between contacts	 1500VAC 50/60HZ (1 minute) 1000VAC 50/60HZ (1 minute)
Insulation Resistance	100 MΩ Min. (500VDC)
Max. ON/OFF Switching Mechanically Electrically	 300 operation/min 30 operation/min
Ambient Temperature	-40°C to +85°C
Operating Humidity	45 to 85% RH
Vibration Endurance Error Operation	 10 to 55Hz Double Amplitude 1.5mm 10 to 55Hz Double Amplitude 1.5mm
Shock Endurance Error Operation	 100G Min. 10G Min.
Life Expectancy Mechanically Electrically	 10^7 operations. Min. (no load) 10^5 operations. Min. (at rated coil voltage)
Weight	abt. 10grs.

9.REFERENCE DATA

Coil Temperature Rise

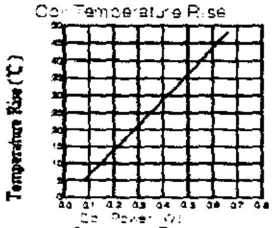

Operation Time

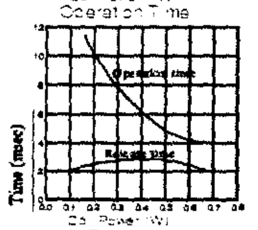

Life Expectancy

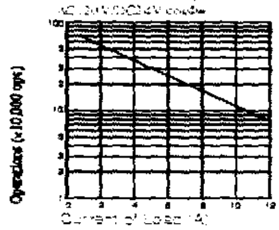

Life Expectancy

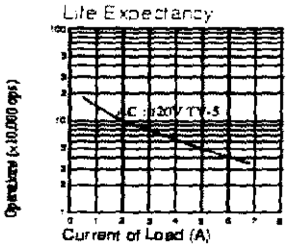

Appendix F.4 Capacitor

SPECIFICATIONS										
Rated voltage	-40~-85℃									
Capacitance	−20%									
Dissipation Factor(20℃, 120Hz)	Rated Voltage(v)	6.3	10	16	25	35	50	63	100	160
	Tan δ	0.24	0.24	0.2	0.2	0.16	0.14	0.12	0.1	0.15
Leakage current:	≤ 0.03cv or 3μA whichever is greater (at 20℃,after 5 minutes)									

LOAD LIFE(85℃)	2000 hours(Polarity inverts for every 250 hours)	
	Leakage current	Not more than the specified value
	Capacitance change	Within~-20% of the initial value
	Dissipation factor	Not more then 150%of the specified value

Temperature Stability(120Hz)	Rated voltage(V)		6.3	10	16	25	35	50	63	100	160
	Impedance ratio	Z-25℃/Z+20℃	4	3		2					4
		Z-40℃/Z-20℃	10	8	6	4	3				-

SHELF LIFE(85℃)	1000hours No voltage applied .They meet the specified value for load life characteristics listed above

DIMENSIONS OF CDLLG SERIES

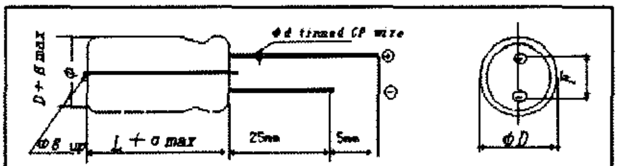

ΦD	5	6.3	8	10	12.5	16	18
Φd	0.5	0.5	0.6	0.6	0.6	0.8	0.8
P	2.0	2.5	3.5	5.0	5.0	7.5	7.5

MULTIPLIER FOR RIPPLE CURRENT

Frequency correction factor for ripple current

Rated Voltage	50.60	120	1K	10K	100K
6.3-16	0.8	1	1.1	1.2	1.2
25-35-	0.8	1	1.5	1.7	1.7
50-160	0.8	1	1.6	1.9	1.9

Case Size DxL(mm)

WV/V / Cap/μF	6.3	10	16	25	35	50	63	100	160V	250
0.1						5x11		5x11		
0.22						5x11		5x11		
0.33						5x11		5x11		
0.47						5x11		5x11		
1						5x11		5x11	6.3x12	6.3x12
2.2						5x11	5x11	5x11	8x12	8x12
3.3						5x11	5x11	6.3x11	10x12	10x12
4.7				5x11	5x11	5x11	5x11	6.3x11	10x16	10x16
10			5x11	5x11	5x11	6.3x11	6.3x11	8x11.5	10x20	12.5x20
22		5x11	6.3x11.4	5x11	6.3x11	6.3x12	8x11.5	10x16	12.5x20	12.5x25
33	5x11	5x11	5x11	6.3x11	6.3x11	8x12.5	10x12.5	10x20	12.5x25	
47	5x11	5x11	6.3x11	6.3x11	8x11.5	10x12.5	10x16	12.5x20	16x25	
100	6.3x11	6.3x11	8x11.5	8x12.5	20x12.5	10x20	12.5x20	16x25	18x35.5	
220	8x11.5	8x11.5	10x12.5	10x16	10x20	12.5x20	16x25	18x35.5		
330	8x11.5	10x12.5	10x16	10x20	12.5x20	12.5x25				
470	10x12.5	10x16	10x20	12.5x20	12.5x25	16x25				
1000	10x20	12.5x20	12.5x25	16x25	16x31.5					
2200	12.5x20	16x25	16x31.5							
3300	16x25	16x31.5								
4700	16x31.5	18x35.5								

Appendix F.5 Result of the signal circuit

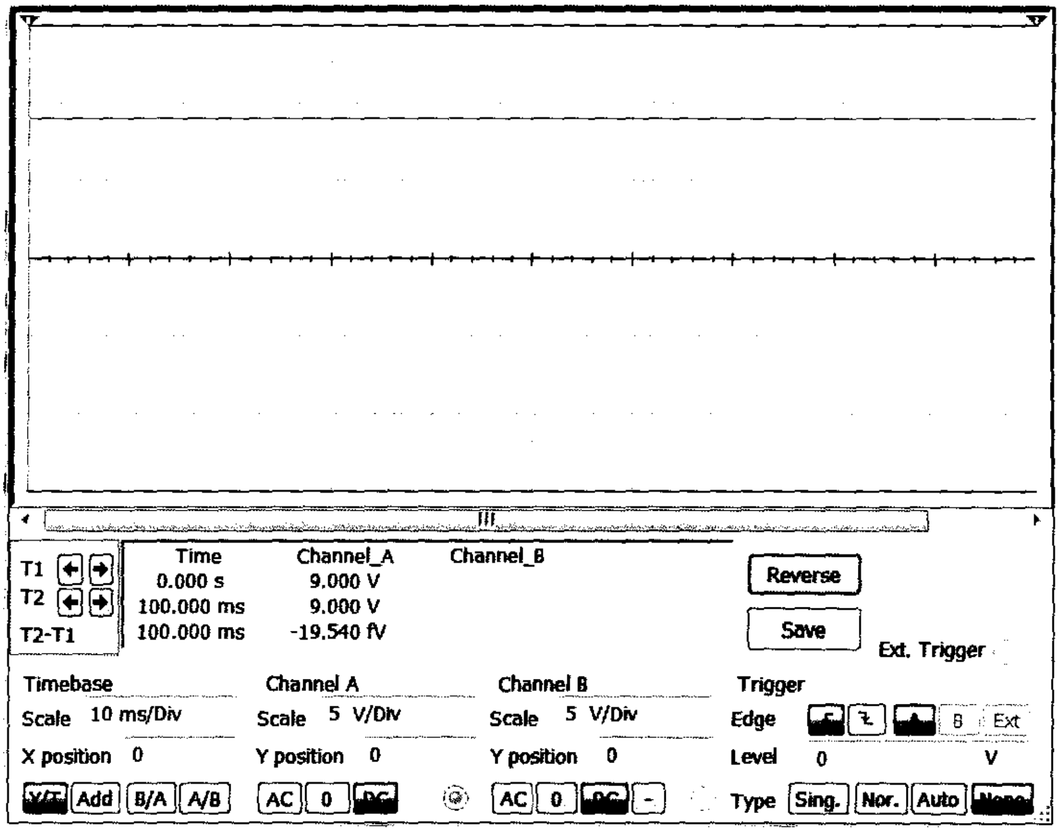

APPENDIX G

BOLTS AND NUTS THAT HAVE BEEN USED

Appendix G.1 Bolts and nuts

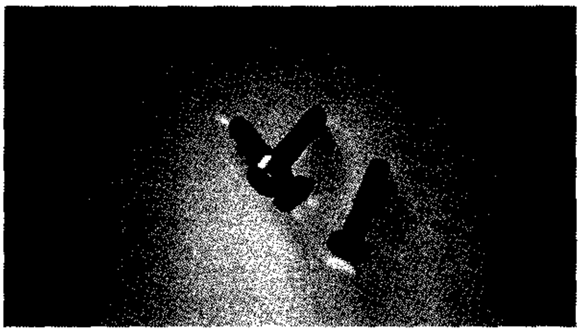

M6 Hexagonal head and allen key bolt

Washers that used to attach flywheel

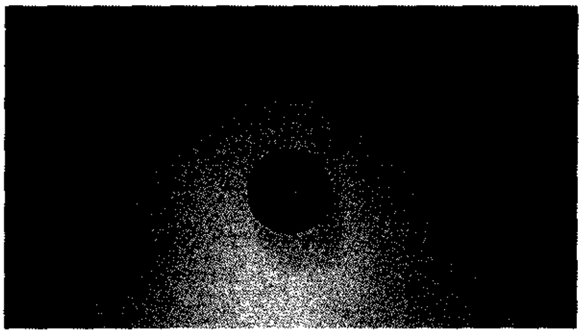

Rubber washer that placed inside flywheel

M9 hexagonal head bolt and nut

APPENDIX H

MACHINES THAT HAVE BEEN USED

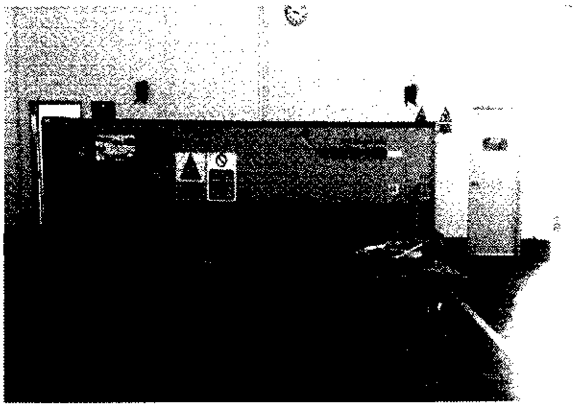

Shear machine

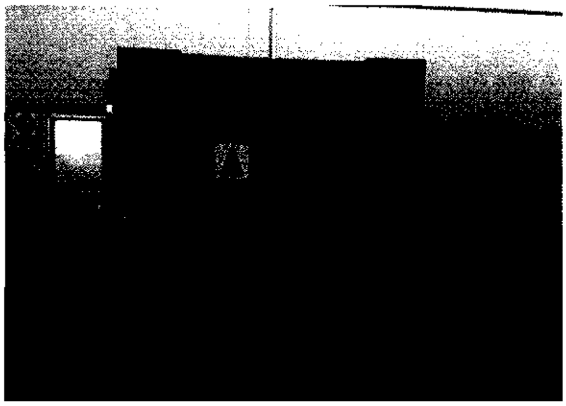

Bending machine

Vertical drilling machine

Milling machine

APPENDIX I

PICTURES THAT WERE TAKEN DURING EXPERIMENT

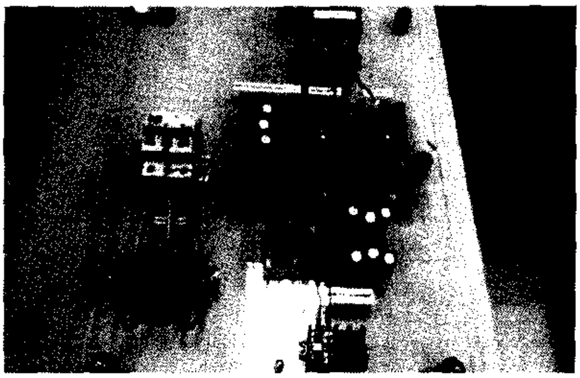

Power transferring circuit

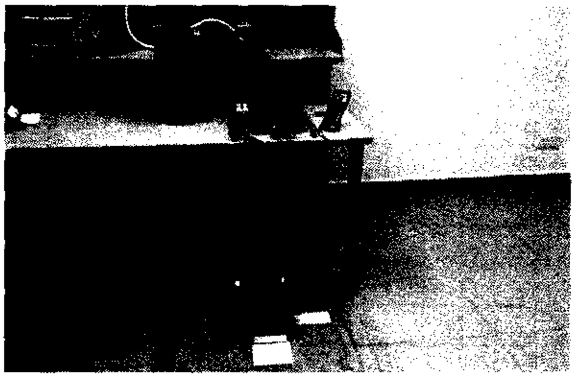

Assembled FESS

Tachometer is recording rpm of flywheel

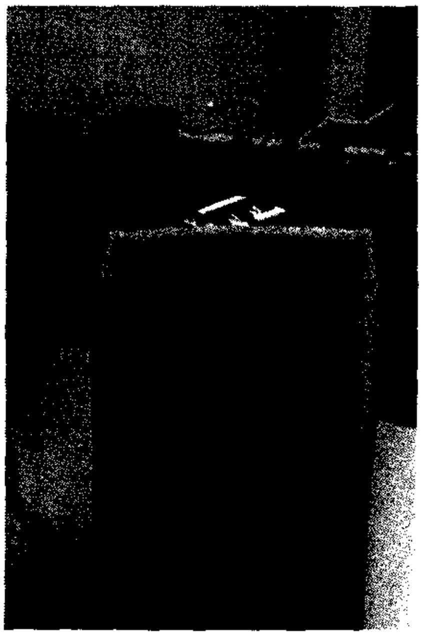

Generated voltage is shown in multimeter

APPENDIX J

GANTT CHART

Purpose	FYP I															FYP II															
Timeline	Sept			Oct				Nov			Dec					Feb		Mar				Apr				May				June	
Week	1	2	3	4	5	6	7	8	9	10	11	12	13	14		1	2	3	4	5	6	7	8	9	10	11	12	13	14	15	16
Task																															
Identify Research Title	■																														
Research Titer Review	■	■																													
Literature View on Title		■	■	■	■	■	■	■	■	■	■																				
Research Scope and Objectives				■	■																										
Research Methodology					■	■	■	■	■	■	■	■																			
Proposal Writing									■	■	■	■																			
Submission of Proposal													■																		
FYP I Presentation														■																	
Preparation for FYP II															■																
Preparation for Raw Material															■	■	■	■	■	■	■	■									
Machining Operation																							■	■	■	■	■				
Test Signal Circuit																		■	■	■	■										
Construct Power Transferring Circuit																					■	■	■	■							
Construct Generator Circuit																								■	■	■	■				
Completion of Mechanical Part																						■	■	■	■	■	■				
Combine Mechanical & Electrical Part																											■	■			
Run Experiment																										■	■	■	■		
Result & Discussion																											■	■	■		
Completion of Project Report																												■	■	■	■
Correction & Submission of Report																														■	■